AWARD NUMBER: W81XWH-17-1-0483

TITLE: Pharmacologic Inhibition of Lipogenesis Suppresses AR and Its Splice Variants to Inhibit Progression of Castration-Resistant Prostate Cancer

PRINCIPAL INVESTIGATOR: Massimo Loda, MD

CONTRACTING ORGANIZATION: Joan and Sanford I. Weill Medical College of Cornell University

REPORT DATE: JANUARY 2022

TYPE OF REPORT: Final Report

PREPARED FOR: U.S. Army Medical Research and Development Command
Fort Detrick, Maryland 21702-5012

REPORT DOCUMENTATION PAGE

Form Approved
OMB No. 0704-0188

1. REPORT DATE	2. REPORT TYPE	3. DATES COVERED
JANUARY 2022	FINAL	09/30/2017 - 09/29/2021

4. TITLE AND SUBTITLE

Pharmacologic Inhibition of Lipogenesis Suppresses AR and Its Splice Variants to Inhibit Progression of Castration-Resistant Prostate Cancer

5a. CONTRACT NUMBER
W81XWH-17-1-0483

5b. GRANT NUMBER

5c. PROGRAM ELEMENT NUMBER

5d. PROJECT NUMBER

5e. TASK NUMBER

5f. WORK UNIT NUMBER

6. AUTHOR(S):

Massimo Loda(mloda@med.cornell.edu), Scott Dehm (dehm@umn.edu), Stephen Plymate (splymate@uw.edu), and Caroline Ribeiro (car4001@med.cornell.edu)

7. PERFORMING ORGANIZATION NAME(S) AND ADDRESS(ES)

Joan and Sanford I. Weill Medical College of Cornell University
University of Washington
University of Minnesota

8. PERFORMING ORGANIZATION REPORT NUMBER

9. SPONSORING / MONITORING AGENCY NAME(S) AND ADDRESS(ES)

U.S. Army Medical Research and Development Command
Fort Detrick, Maryland 21702-5012

10. SPONSOR/MONITOR'S ACRONYM(S)

11. SPONSOR/MONITOR'S REPORT NUMBER(S)

12. DISTRIBUTION / AVAILABILITY STATEMENT

Approved for Public Release; Distribution Unlimited

13. SUPPLEMENTARY NOTES

14. ABSTRACT

A hallmark of prostate cancer progression is dysregulation of lipid metabolism via overexpression of fatty acid synthase (FASN), a key enzyme in the *de-novo* fatty acids synthesis. Metastatic castration-resistant prostate cancer (mCRPC) develops resistance to inhibitors of androgen receptor (AR) signaling through a variety of mechanisms, including the emergence of the constitutively active AR variant V7 (AR-V7). We used a novel FASN inhibitor (IPI-9119) and demonstrated that selective FASN inhibition antagonizes CRPC growth through metabolic reprogramming and results in reduced protein expression and transcriptional activity of both full-length AR (AR-FL) and AR-V7. Activation of the reticulum endoplasmic stress response resulting in reduced protein synthesis was involved in IPI-9119-mediated inhibition of the AR pathway. *In vivo*, IPI-9119 reduced growth of AR-V7-driven CRPC xenografts and human mCRPC-derived organoids, and enhanced the efficacy of enzalutamide in CRPC cells. These findings provide a rationale for the use of FASN inhibitors in CRPCs, including those overexpressing AR-V7.

15. SUBJECT TERMS

IPI-9119, fatty acid synthase, de novo lipogenesis, androgen receptor, AR-V7

16. SECURITY CLASSIFICATION OF:			17. LIMITATION OF ABSTRACT	18. NUMBER OF PAGES	19a. NAME OF RESPONSIBLE PERSON
a. REPORT	b. ABSTRACT	c. THIS PAGE			19b. TELEPHONE NUMBER *(include area code)*
Unclassified	Unclassified	Unclassified	Unclassified	34	USAMRDC

Table of Contents

Page

1.INTRODUCTION

Treatment of metastatic castration-resistant prostate cancer (mCRPC) mostly relies on second-generation anti-androgens agents, such as enzalutamide or abiraterone, which have greatly improved quality of life and survival of patients [1-3]. However, most patients eventually progress to treatment-refractory metastatic disease [4]. Despite castrate levels of circulating androgens in patients on androgen deprivation therapy, persistent activation of the androgen receptor (AR) axis still drives mCRPC [5]. Different mechanisms of resistance to AR-directed therapies have been described, including the emergence of AR splice variants (AR-Vs), such as AR-V7 [6-8]. AR-V7 lacks the C-terminal ligand-binding domain of full-length AR (AR-FL) and functions as a constitutively active, ligand-independent transcription factor that drives growth of mCRPC cells *in vitro* and *in vivo* [9]. AR-V7 mRNA and protein are up-regulated in mCRPC bone metastases [10] and associated with a decrease in overall survival [11] and resistance to Enza and/or Abi treatment [12].
In contrast to normal prostatic cells that rely mostly on diet-derived lipids for fatty acids (FA), prostate cancer (PCa) progression is marked by increasing rates of *de-novo* FA synthesis, independent of circulating lipid levels [13]. The key enzyme, fatty acid synthase (FASN), catalyzes the synthesis of palmitate from malonyl-CoA and acetyl-CoA using NADPH as the reducing agent. The expression of enzymes in the lipogenic pathway, including FASN, and transcriptional regulators such as the sterol regulatory element-binding proteins (SREBPs) is significantly increased in PCa, especially in the mCRPC setting [14-16]. Besides providing structural lipids and bioenergetics to sustain cancer cell growth, enhanced FASN activity is also accompanied by activation of the PI3K/Akt/mTORC1 pathway, palmitoylation of known oncogenes including k-RAS and WNT-1, regulation of endoplasmic reticulum function to sustain membrane biogenesis [13, 17], and resistance to genotoxic insults [18].
Inhibition of FASN activity through genetic and pharmacological means suppresses PCa cell growth by cell cycle arrest and/or apoptosis [13], while FASN overexpression is linked to resistance to chemotherapy [18]. FASN expression is transcriptionally induced by AR through the activation of SREBP1 [19] or by a direct binding to FASN promoter regions [20]. However, the evidence that SREBP1 inhibition can downregulate AR-FL [21] suggests a mutual regulation between AR signaling and FA metabolism.

2.KEYWORDS

Prostate cancer, castration-resistant prostate cancer (CRPC), lipogenesis, AR signaling, AR-V7, fatty acid synthase (FASN), metabolomics, ER stress.

3.ACCOMPLISHMENTS

- What were the major goals of the project?

The major goals of this project were to: 1) evaluate the therapeutic benefit of inhibiting *de novo* lipogenesis in preclinical models of prostate cancer (*in vitro* and *in vivo*), with a particular attention to castration resistant prostate cancer (CRPC); 2) evaluate the metabolic effects of fatty acid synthase (FASN) inhibition in CRPC; 3) evaluate the therapeutic benefit of combining inhibitors of *de novo* lipogenesis and AR signaling inhibitors; 4) understand the underpinning molecular mechanisms of FASN inhibitors activity; 5) evaluate the expression of FASN, AR-FL and AR-V7 in human metastatic prostate cancer; 6) characterize the mechanism of AR downregulation following FASN inhibition; 7) determine how *de novo* lipogenesis inhibition affects DNA damage response; 8) evaluate if targeting FASN enhances efficacy of PARP inhibition therapy in CRPC; 9) evaluate the effects of FASN inhibition in the lipidome of prostate cancer cells; 10) characterize lipidome in patient-derived xenograft (PDX) model; 11) characterize the energetic profile and metabolic adaptation induced by FASN blockade; 12) assess the impact of FASN blockade in cell bioenergetic and energy source;

- What was accomplished under these goals?

A) The major activities of this project were:

1. Evaluate the therapeutic efficacy of FASN inhibitor IPI-9119 using *in-vitro* CRPC models, in CRPC xenograft models, and in patient-derived organoids.
2. Evaluate the effect of FASN inhibitor IPI-9119 on tumor transcriptome using *in vitro* models.
3. Evaluate the effect of FASN inhibitor IPI-9119 on tumor metabolome using *in vitro* models.

4. Evaluate the mechanisms linking FASN activity suppression and AR pathway inhibition.
5. Evaluate the effect of FASN inhibitor IPI-9119 on the androgen receptor transcriptional activity.
6. Evaluate the expression of FASN and androgen receptor (AR-FL and AR-V7) in human cases of metastatic prostate cancer.
7. Evaluate how FASN inhibition through IPI-9119 downregulates AR and AR-V7 levels in CRPC models.
8. Evaluate the synergistic effect of FASN inhibition with other therapies, such as PARP inhibition and AR antagonists, in CRPC models.
9. Evaluate the effect of FASN inhibitor IPI-9119 on tumor lipidome using *in vitro* models.
10. Evaluate lipidome of different PDX models and correlate with gene alterations.
11. Evaluate CRPC cells adaptation and bioenergetics following FASN inhibition.

B) The specific objectives of this project were:

1. Evaluate the effect of FASN inhibitor IPI-9119 on tumor growth/ cell cycle/ apoptosis in preclinical models of androgen-sensitive castration resistant prostate cancer and patient-derived organoids (Dana-Farber Cancer Institute site /PI: Loda/ Partners site /PI: Plymate).
2. Perform RNA-seq to evaluate the effect of FASN inhibition on tumor transcriptome (Dana-Farber Cancer Institute site /PI: Loda/ Partners site /PI: Plymate).
3. Perform metabolomics to evaluate the effect of FASN inhibition on tumor metabolome Dana-Farber Cancer Institute site /PI: Loda).
4. Evaluate the mechanisms linking FASN activity suppression and AR pathway inhibition (Dana-Farber Cancer Institute site /PI: Loda/ Partners site /PI: Dehm).
5. Evaluate the effect of FASN inhibitor IPI-9119 on the androgen receptor transcriptional activity. (Dana-Farber Cancer Institute site /PI: Loda/ Partners site /PI: Plymate; PI: Dehm).
6. Explore opportunities for therapy with IPI-9119 in the clinical metastatic prostate cancer setting by characterizing FASN and androgen receptor expression in human cases of advanced disease. (Dana-Farber Cancer Institute site /PI: Loda/ Partners site /PI: Plymate).
7. Evaluate the effect of FASN inhibitor IPI-9119 on AR and AR-V7 degradation through proteasome in castration resistant prostate cancer, also characterizing receptor dimerization role by AR-V7 overexpression in AR-null cell lines (Weill Cornell Medical College /PI: Loda).
8. Assess how FASN inhibition through IPI-9119 can potentiate anti-tumor efficacy of the antagonist of the androgen receptor Enzalutamide in 3D organoid models of CRPC (Weill Cornell Medical College /PI: Loda).
9. Determine the effect of FASN activity suppression by IPI-9119 in DNA damage repair (DDR) pathway modulation, using RNAseq data analysis, western blot characterization of key enzymes in DDR pathways and a proposed mechanism that involves sphingolipid metabolism upregulation (Weill Cornell Medical College /PI: Loda).
10. Evaluate the lipid remodeling caused by FASN inhibition in both androgen sensitive and CRPC cell lines (Partners site /PI: Dehm).
11. Characterize the lipid profiling of different PDX models and relative gene expression of lipid modifying enzymes (Partners site /PI: Plymate).
12. Characterize how FASN inhibition alters respiration and mitochondria function in CRPC cells (Weill Cornell Medical College /PI: Loda).

C) Significant results and key outcomes:

<u>1. FASN inhibition blocks cell growth and induces apoptosis</u>
As described in **SOW for year 1 (months 1-12)**, we further characterized FASN activity under treatment with IPI-9119 and analyzed cell growth, cell cycle kinetics, and apoptosis across a panel of AR-positive, androgen-dependent (AD) (LNCaP), androgen independent (AI) (C4-2, C4-2B, LNCaP-Abl) and Enza/Abi-resistant AI cell lines harboring the AR-V7 splice variant (22Rv1, LNCaP-95). IPI-9119 inhibited cell growth and clonogenic survival in PCa cell lines **(Figure 1A-B, representative images).** Cell growth inhibition by IPI-9119 was rescued by the addition of exogenous palmitate, confirming that the effects on cell growth and survival were due to on-target activity and that palmitate rather than the toxic accumulation of malonyl-CoA accounts for IPI-9119-

mediated anti-cancer effect (**Figure 1C**). IPI-9119 reduced the proportion of S-phase cells and increased that of G0/G1- and sub-G1-phase cells (**Figure 1D**), and decreased expression of cyclin A2 (**Figure 1E**). Analysis of Parp cleavage, Annexin V, and propidium iodide staining showed induction of apoptosis by IPI-9119 (**Figure 1E**).

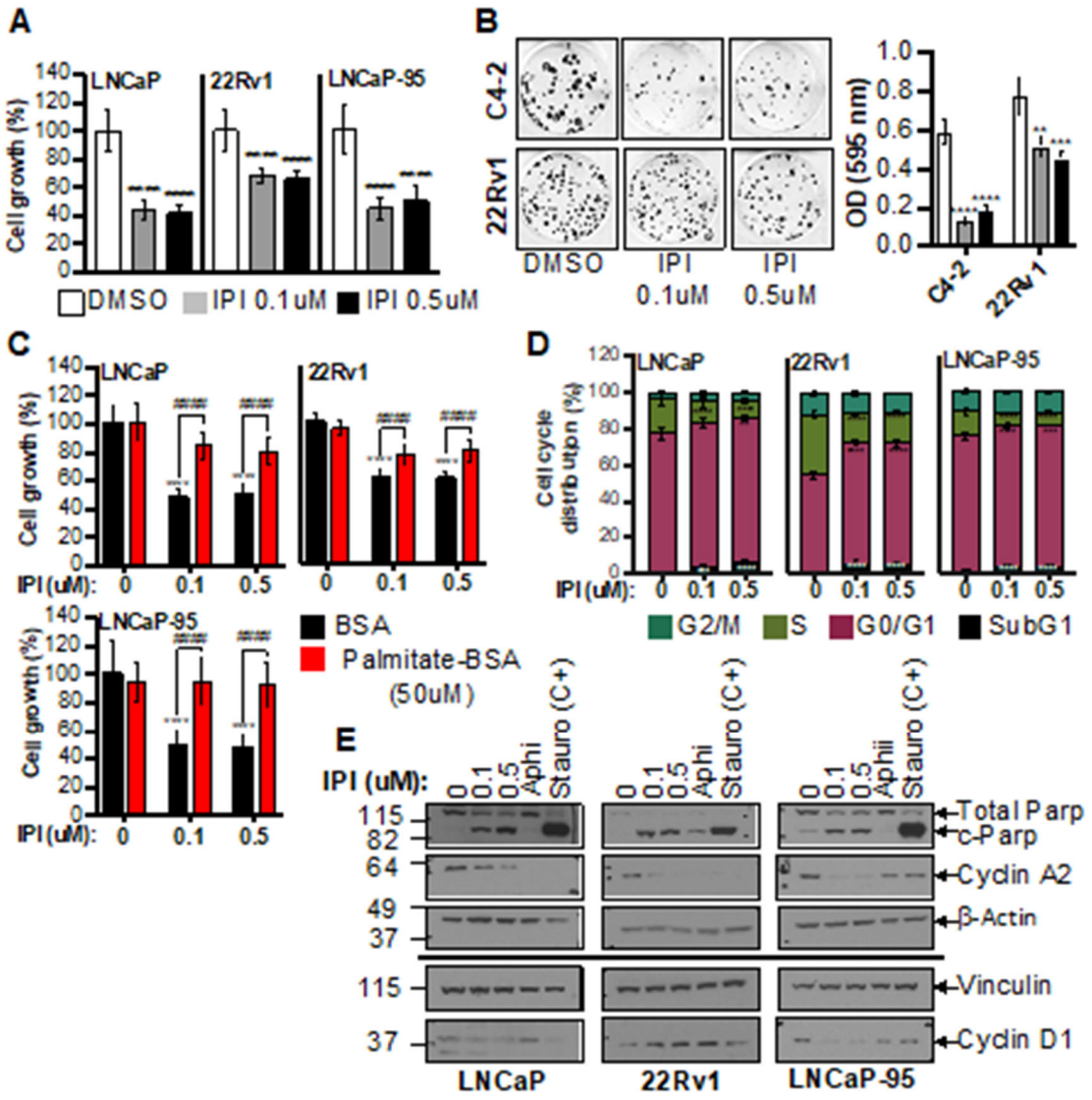

Figure 1. IPI-9119 inhibits PCa cell growth and induces cell cycle arrest and apoptosis.

A) Measurement of cell growth after 6-day treatment with IPI-9119 (IPI). Data are expressed as the mean number of viable cells ± SD and plotted as % DMSO. ****p<0.0001, one-way ANOVA followed by Tukey's post hoc test. (**B**) Clonogenic assay, following 3-week treatment with IPI or DMSO. Representative images of colony formation (left) and quantification (right). Data are expressed as the mean optical density (OD) ± SD (n. **p<0.01, ***p<0.001, ****p<0.0001, one-way ANOVA followed by Tukey's post hoc test. (**C**) Cell growth rescue by exogenous palmitate. Data are expressed as the mean growth ± SD (n/concentration= 9) and plotted as % DMSO. ****p<0.0001 IPI *vs* DMSO, $^{\#\#\#\#}$p<0.0001 IPI+palmitate *vs* IPI, two-way ANOVA followed by Sidak's post hoc test. (**D**) Flow cytometry using propidium iodide (PI) and bromodeoxyuridine (BrDU), following IPI treatment (6 days). Data are expressed as the mean % ± SD (n=6). **p<0.01, ***p<0.001, ****p<0.0001, two-way ANOVA followed by Sidak's post hoc test. (**E**) Representative immunoblotting of cell cycle and apoptosis markers. Experiment was repeated twice. S-phase inhibitor aphidicolin (Aphi, 0.3 ug/ml, 3 hrs) and the apoptosis inducer staurosporine (Stauro, 1uM for 24 hrs) were used as positive controls.

No growth inhibition by IPI-9119 was observed in FASN knockout (KO) PCa cells (**Figure 2A,B**), confirming the specificity of IPI-9119 for FASN. Moreover, the anti-tumor effect of IPI-9119 was preserved in culture medium with whole serum compared to lipid-reduced serum (**Figure 2C**).

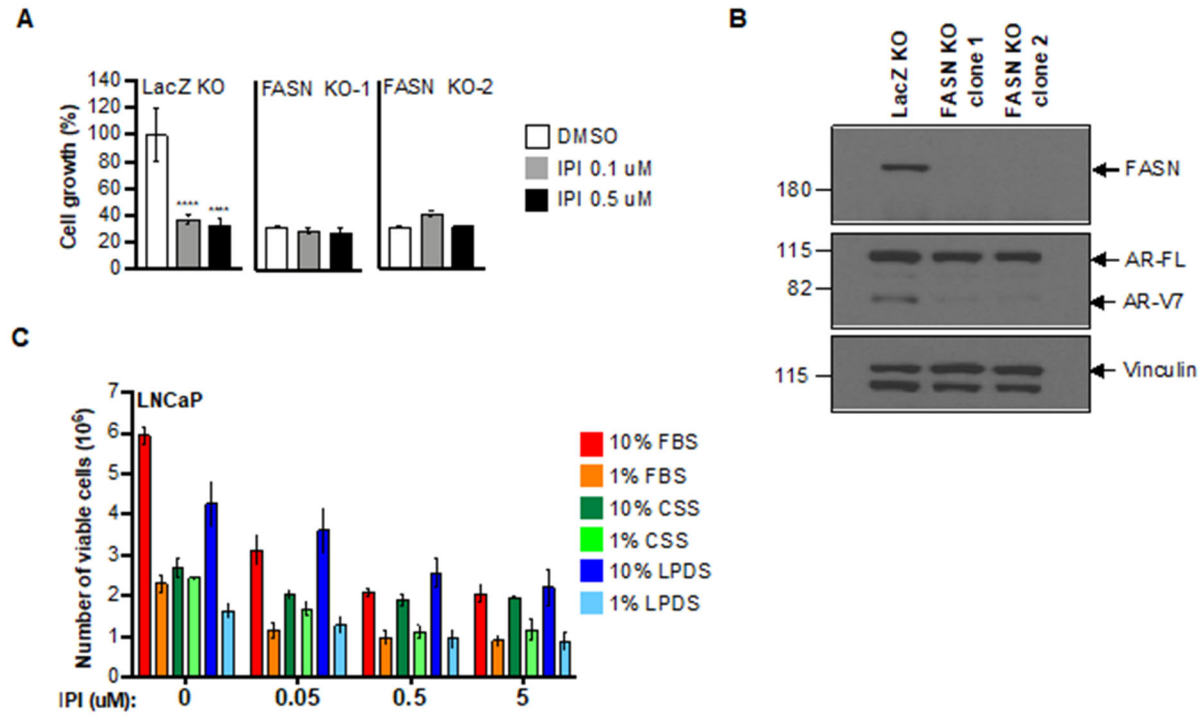

Figure 2. **IPI-9119 specifically inhibits FASN-mediated cell growth in PCa cells.**
(**A**) Cell growth of FASN KO-1 (clone 1) and KO-2 (clone 2) LNCaP-95 and control (Lac Z KO) cells, following treatment with IPI for 6 days. Data are expressed as the mean number of viable cells ± SD (n/concentration= 3), and plotted as % DMSO of Lac Z KO cells. ****p<0.0001 IPI *vs* DMSO, two-way ANOVA followed by Sidak's post hoc test. (**B**) Immunoblotting showing the complete absence of FASN in single FASN KO clones (1 and 2). (**C**) Effect of different media on IPI efficacy. Cell growth was assessed after 6 days of treatment with IPI in the presence of different sera composition and % in the media. FBS: fetal bovine serum; CSS: charcoal stripped serum; LPDS: lipoprotein depleted serum. Data are expressed as the mean ± SD of 9 independent samples (n=9).

Following the preliminary preclinical data included in the grant proposal, as stated in the SOW for year 1 (months 3-30), we started testing the effect of FASN inhibitor IPI-9119 in other CRPC. We utilized LNCaP-95 xenograft, a model of CRPC resistant to Enza and/or Abi. LNCaP-95-bearing xenografts were exposed to IPI-9119 with a constant infusion (0.5 µl/hr; 100 mg/ml) for 4 weeks, using a subcutaneous osmotic ALZET pump. Mice did not show any signs of toxicity, stress, weight loss (**Figure 3A**) or changes in feeding behavior. We observed significant inhibition of xenograft tumor growth at the end of the treatment (33% inhibition-end of treatment; p<0.0016, Mann-Whitney test) (**Figure 3B**), with concomitant intra-tumoral inhibition of FASN activity (**Figure 3C**). Finally, we tested the efficacy of IPI-9119 in MSK-PCa3, a published and publicly available CRPC patient-derived organoid model, which is a FASN and AR-FL positive human mCRPC organoid line (13). An equal number of cells were plated and organoids were grown for 25 days. We observed significant reduction in organoid growth under treatment with IPI-9119 (**Figure 3D**), confirming the anti-tumorigenic effect of FASN inhibition in human mCRPC.

.

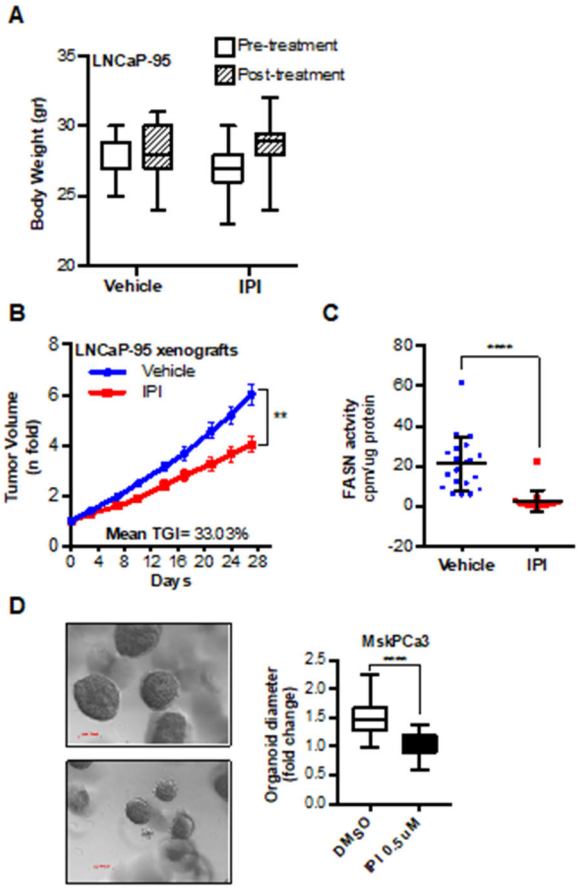

Figure 3. **IPI-9119 specifically inhibits FASN-mediated cell growth in PCa cells.**
(**A**) Mouse body weight under treatment with IPI-9119 (IPI) using subcutaneous pump infusion for four weeks. (**B**) Average tumor volume of LNCaP-95 xenografts during 28-day treatment with IPI-9119 (IPI) using the ALZET subcutaneous pump infusion (n=20 vehicle, n=17 IPI). Results are expressed as n fold the mean initial volume (equal to 1) ± SEM. (**p= 0.0016, end of treatment, Mann-Whitney non-parametric test). (**C**) Measurement of FASN activity in LNCaP-95 xenografts homogenates collected at the end of treatment. Results are expressed as cpm normalized to protein content ± SD ****p<0.0001, Mann-Whitney non-parametric test. (**D**) Representative image of MSK-PCa3 organoids treated with IPI or DMSO for 25 days (left). Statistical analysis of the organoids sizes (right). Diameters of organoids treated with IPI were compared to DMSO (n= 78 DMSO-treated, n= 95 IPI-treated), ****p<0.0001, Student t-test. Pixel magnification is indicated.

Site of performance: Dana-Farber Cancer Institute/ University of Washington
DFCI site team: Massimo Loda (PI), Giorgia Zadra (Co-investigator), Leigh Ellis (Co-investigator), Caroline F. Ribeiro (Post-doctoral fellow).
Partners site team: Stephen Plymate (co-PI), Cynthia Sprenger (co-investigator), Shihua Sun, Kathryn Epilepsia, Gang Liu, Yan Wang.

2. FASN inhibition alters the PCa transcriptome

As described in **SOW for year 1 (months 1-12),** we performed RNA-seq in AD LNCaP and AI (22Rv1 and LNCaP-95) to explore the effect of FASN inhibitor IPI-9119 on the tumor transcriptome. This analysis revealed broad upregulation of key lipogenic genes suggesting a compensatory mechanism to inhibition of FASN activity (**Figure 4**).

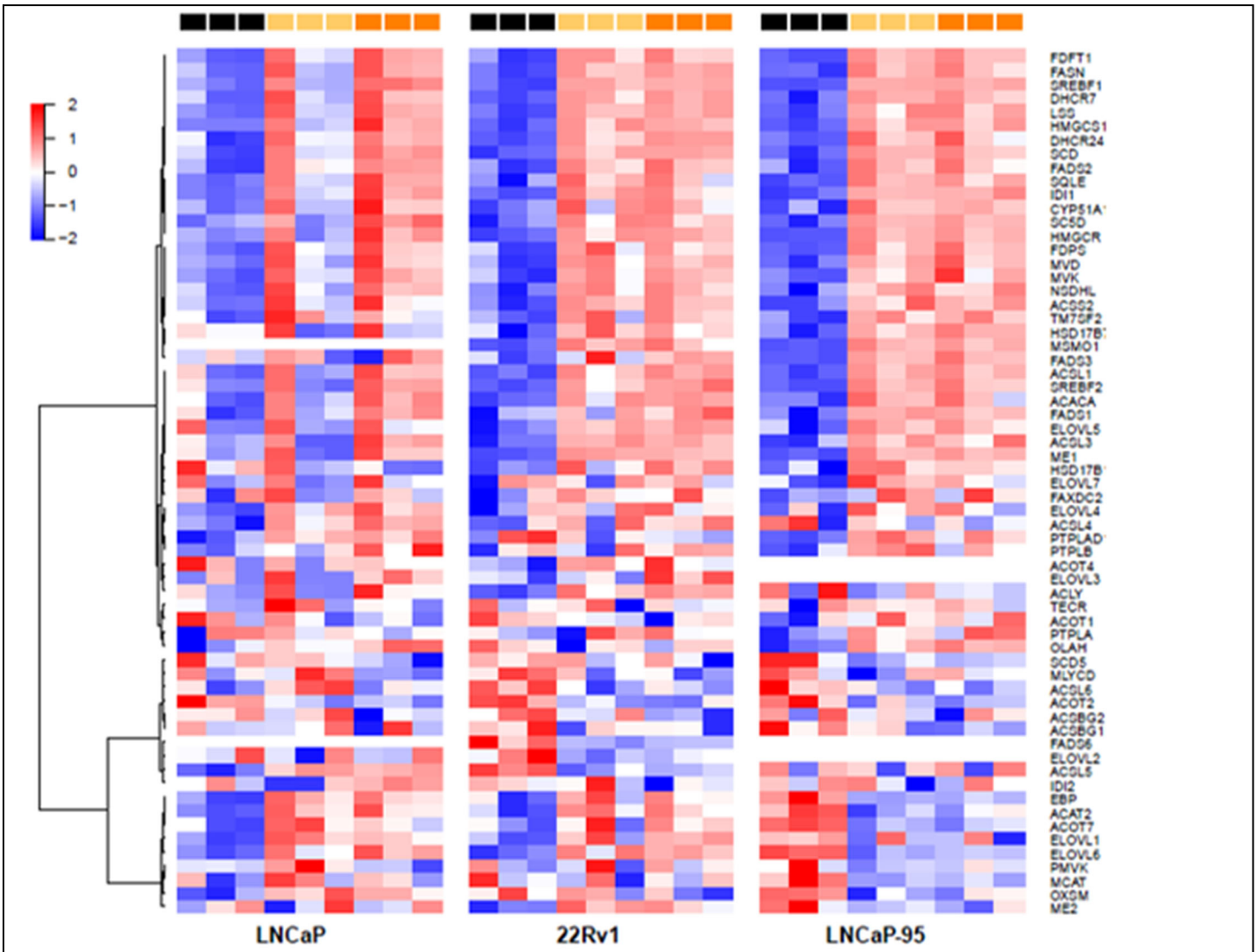

Figure 4. Expression of key genes of lipid metabolism is increased following treatment with IPI-9119. Heatmaps of RNA-seq data showing the expression of key genes involved in lipid metabolism. Normalized counts are shown (n=3).

Site of performance: Dana-Farber Cancer Institute/ University of Washington
DFCI site team: Massimo Loda (PI), Giorgia Zadra (Co-investigator), Leigh Ellis (Co-investigator), Caroline F. Ribeiro (Post-Doctoral fellow).
Partners site team: Stephen Plymate (co-PI), Cynthia Sprenger (co-investigator), Shihua Sun, Kathryn Epilepsia, Gang Liu, Yan Wang.

Moreover, in agreement with metabolomics data (see below), gene set enrichment analysis (GSEA) using RNA-seq data confirmed downregulation of pathways associated with amino-acid and protein translation (i.e., LNCaP cells), as well as purine and pyrimidine synthesis (i.e., 22Rv1 and LNCaP-95 cells) (data not shown), providing the map of a profound metabolic reprogramming induced by FASN inhibition (**Figure 5C**).

3. FASN inhibition alters the PCa metabolome

As stated in the **SOW (months: 3-30**), we analyzed the metabolic consequences of FASN inhibition. Metabolic profiling was performed in cell lysates of LNCaP, 22Rv1, and LNCaP-95 cells exposed to IPI-9119 or DMSO for 6 days. A marked separation of samples treated with IPI-9119 from control groups (independent of the drug concentration) was observed based on the entire metabolic profile (**Figure 5A**). Ninety-one of 418 metabolites were significantly modulated by IPI-919 treatment (both 0.1 and 0.5 μM) in all the cell lines analyzed ($p<0.05$; FDR<0.05) (**Figure 5B**). These included metabolites involved in lipid metabolism as well as amino acid, TCA

cycle, carbohydrate, and nucleotide metabolism. As expected from the suppression of *de-novo* lipogenesis, significant reduction of the two most common FAs derived from palmitate, namely oleic and palmitoleic acids, and accumulation of polyunsaturated FAs (DPA, DHA, EPA, and arachidonate) (**Figure 5C**) were observed. Moreover, enhanced phospholipid remodeling (e.g., decrease in phosphoethanolamine species in favor of phosphatidylcholine) was induced in LNCaP and LNCaP-95 cells (data not shown). Thus, while RNA-seq data

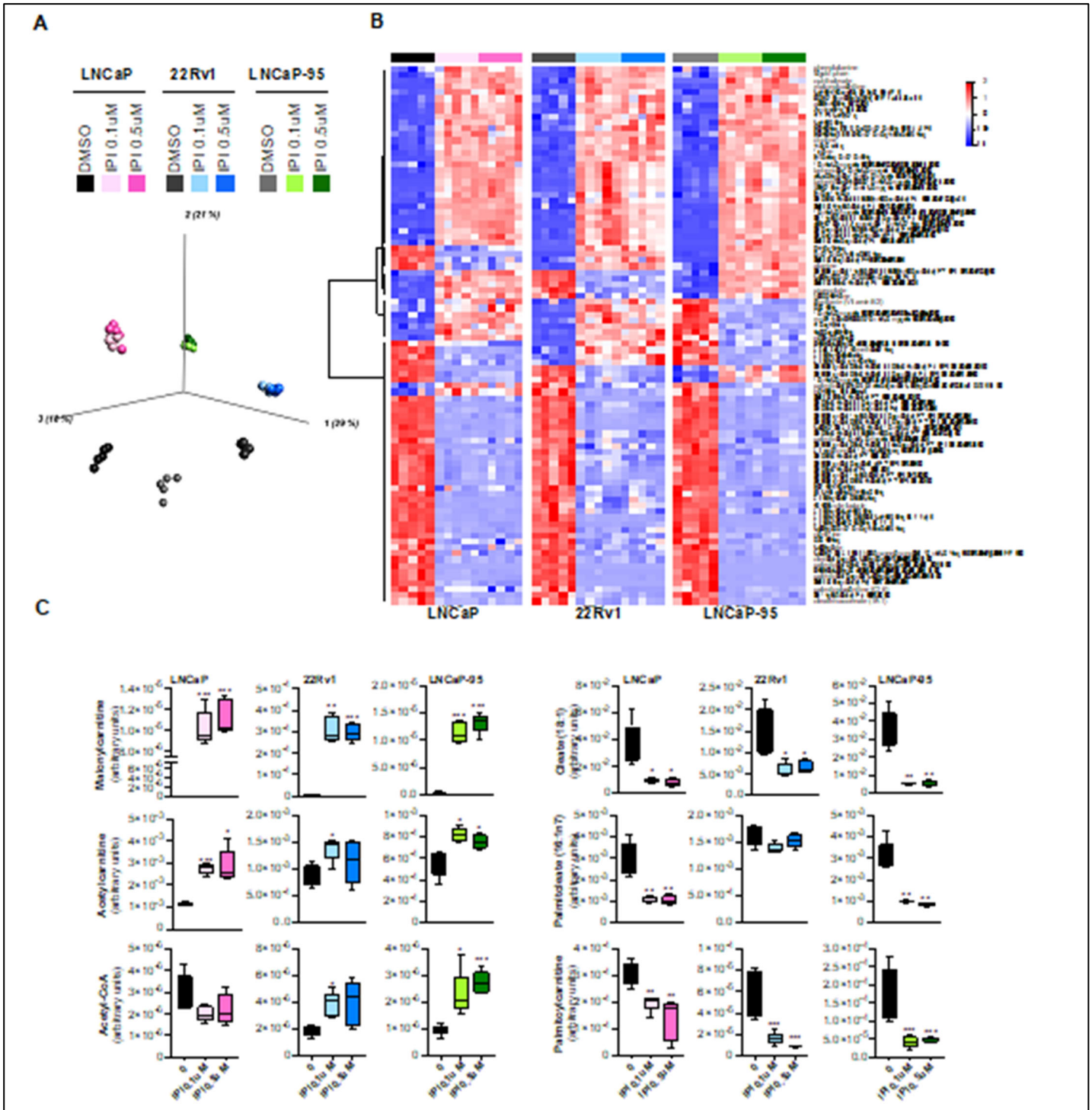

Figure 5. IPI-9119 induces a profound metabolic reprogramming in PCa cells.
(**A**) Principal component analysis of the PCa cell lines analyzed (n= 6/condition). (**B**) Heatmap representing the metabolites significantly altered under IPI treatment at both drug concentrations (0.1 and 0.5 μM) in all the 3 cell lines ($p<0.05$, FDR <0.05). log_2 (normalized values +1) are plotted. (**C**) Box plots showing the levels of key metabolites involved in lipid metabolism from metabolomics data, (n= 6/condition). $^{***}q<0.001$; $^{**}q<0.01$; $^{*}q<0.05$, Student t-test.

highlighted compensatory transcriptional upregulation of FA synthesis genes/regulators by IPI-9119, the intracellular metabolic changes confirmed the suppression of FASN activity.

Following blockade of FA synthesis, unused acetyl-CoA can be redirected towards the cholesterol pathway. Increased intracellular cholesterol levels were detected in all cell lines (**Figure 6A**). Accordingly, GSEA highlighted the upregulation of cholesterol synthesis and steroidogenesis pathways (**Figure 6B**).

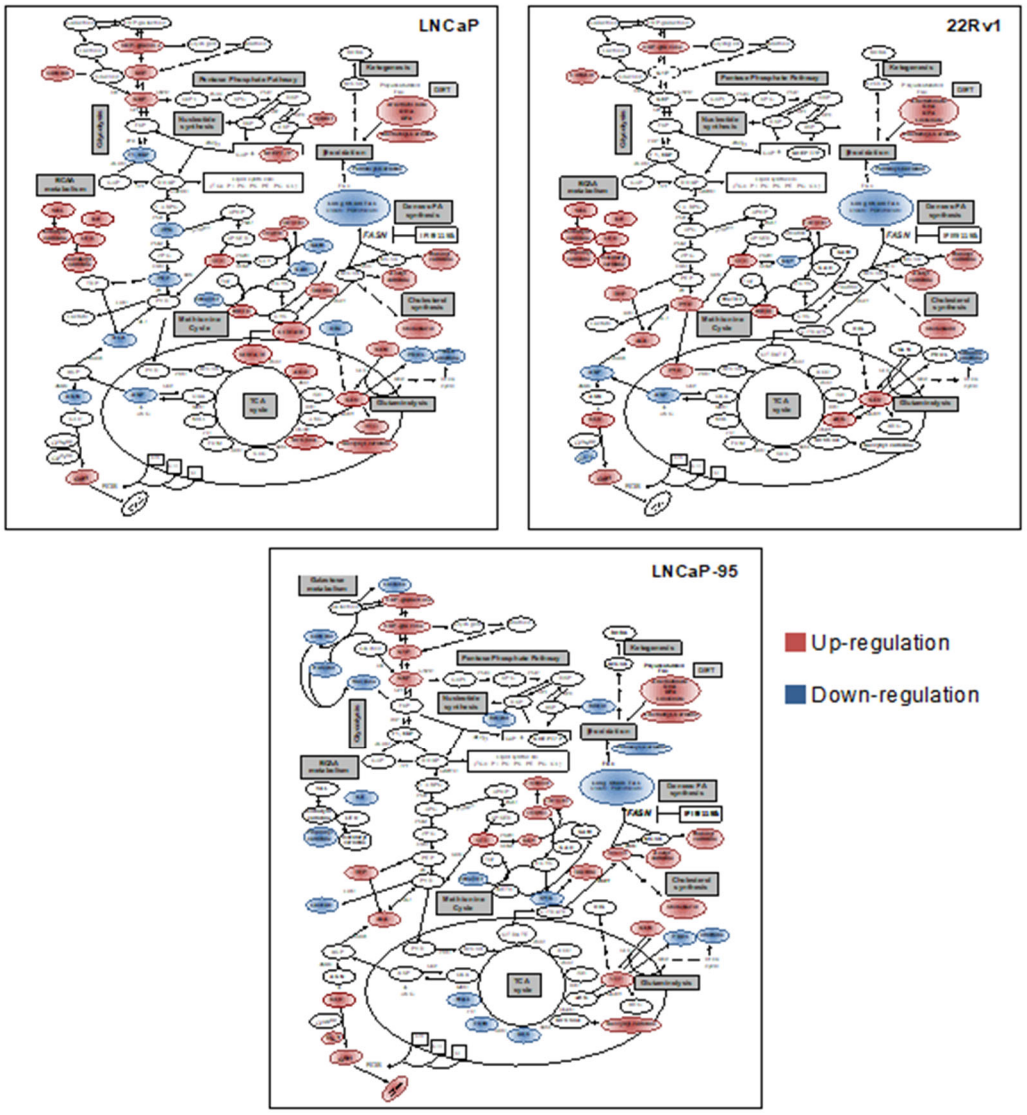

Figure 6. Graphical representation of the key metabolites involved in central carbon metabolism. Metabolites that were significantly increased or decreased under IPI-9119 treatment (6 days) at both the concentration (IPI 0.1 vs DMSO and IPI 0.5 uM vs DMSO, p value <0.05, FDR < 0.05; Student t-test) are depicted in red or blue, respectively (n=6/ condition).

MS-based analyses, however, did not reveal any significant increase in testosterone or dihydrotestosterone levels (data not shown). Alterations in metabolic pathways other than FA synthesis (e.g., glutamine/glutamate, branched-chain amino acids, glycogen metabolism) were observed in a cell-type specific manner (**Figure 7**). These data show that IPI-9119 profoundly alters FA metabolism, affecting both synthetic and catabolic reactions.

Site of performance: Dana-Farber Cancer Institute
DFCI site team: Massimo Loda (PI), Giorgia Zadra (Co-investigator), Leigh Ellis (Co-investigator), Caroline F. Ribeiro (Post-Doctoral fellow).

4. IPI-9119 induces ER stress and AR/AR-V7 protein translation inhibition

In our grant proposal, we showed that FASN inhibition with IPI-9119 reduces AR-FL and AR-V7 proteins. We thus explored the mechanisms underpinning AR-FL/AR-V7 reduction induced by FASN inhibition. It has previously been shown that changes in membrane lipid composition, including increased phosphatidylcholine/ phosphatidylethanolamine ratio and increased free cholesterol levels induce endoplasmic reticulum (ER) stress [22-24]. Our metabolomics data confirmed these alterations following IPI-9119 treatment (data not shown). FASN inhibition-induced ER stress was previously associated with increased phosphorylation of the translation initiation factor eiF2α, reduction in cellular protein synthesis, and induction of apoptosis [17]. Moreover, alteration of calcium (Ca^{2+}) homeostasis induced by the ER stress inducer thapsigargin (Tg) or Ca^{2+} ionophore was reported to inhibit Cap-dependent AR protein synthesis and to induce AR degradation, respectively [25, 26]. Therefore, instead of focusing on the spliceosome (**as stated in the SOW, months 1-12**) we turned our attention on the effect of IPI-9119 on ER stress. Specifically, we assessed whether induction of ER stress was associated with IPI-9119-mediated reduction in AR-FL/AR-V7 protein synthesis and anti-proliferative effects. We confirmed increased phosphorylation of eiF2α starting at 3 days of treatment with IPI-9119, and global protein synthesis reduction (**Figs. 7A and B**). Accordingly, we observed IPI-9119-mediated reduction of protein translation co-factor eiF4B, recently involved in FASN-mediated oncogenic translation [27] (**Figure 7C**). To corroborate the link between induction of ER stress and reduction of AR axis, we used the ER stressor Tg at early time points (12hr) where cell growth inhibition was not evident yet. While Tg induced significant reduction of AR-FL in LNCaP cells, a one-hr pretreatment with an ER stress inhibitor, the Ca^{2+} chelant bapta (20 uM), partially restored its expression. Similar results were obtained when ER stress was inhibited using the PERK inhibitor GSK 2606414 (100 nM, 24 hr) (**Figs. 7D and E**). These results suggest that ER stress is involved in inducing AR pathway downregulation. Finally, addition of exogenous palmitate ameliorates ER stress markers while rescuing both AR/AR-V7 expression (**Figure 7F**) and IPI-9119-induced cell growth inhibition (**Figure 1C**). We confirmed these findings using FASN KO models (data not shown). Altogether, these data suggest the participation of ER stress in mediating the anti-cancer effect of FASN inhibition (**Figure 7G**) in concert with other mechanisms, first and foremost the reduction of lipid membrane synthesis.

Sites of performance: Dana-Farber Cancer Institute, University of Minnesota, Twin Cities
DFCI site team: Massimo Loda (PI), Giorgia Zadra (Co-investigator), Leigh Ellis (Co-investigator), Caroline F. Ribeiro (Post-Doctoral fellow).
U of M site team: Scott Dehm (co-PI), Yeung Louisa Ho (Post-doctoral fellow), Yingming Li (Research Associate)

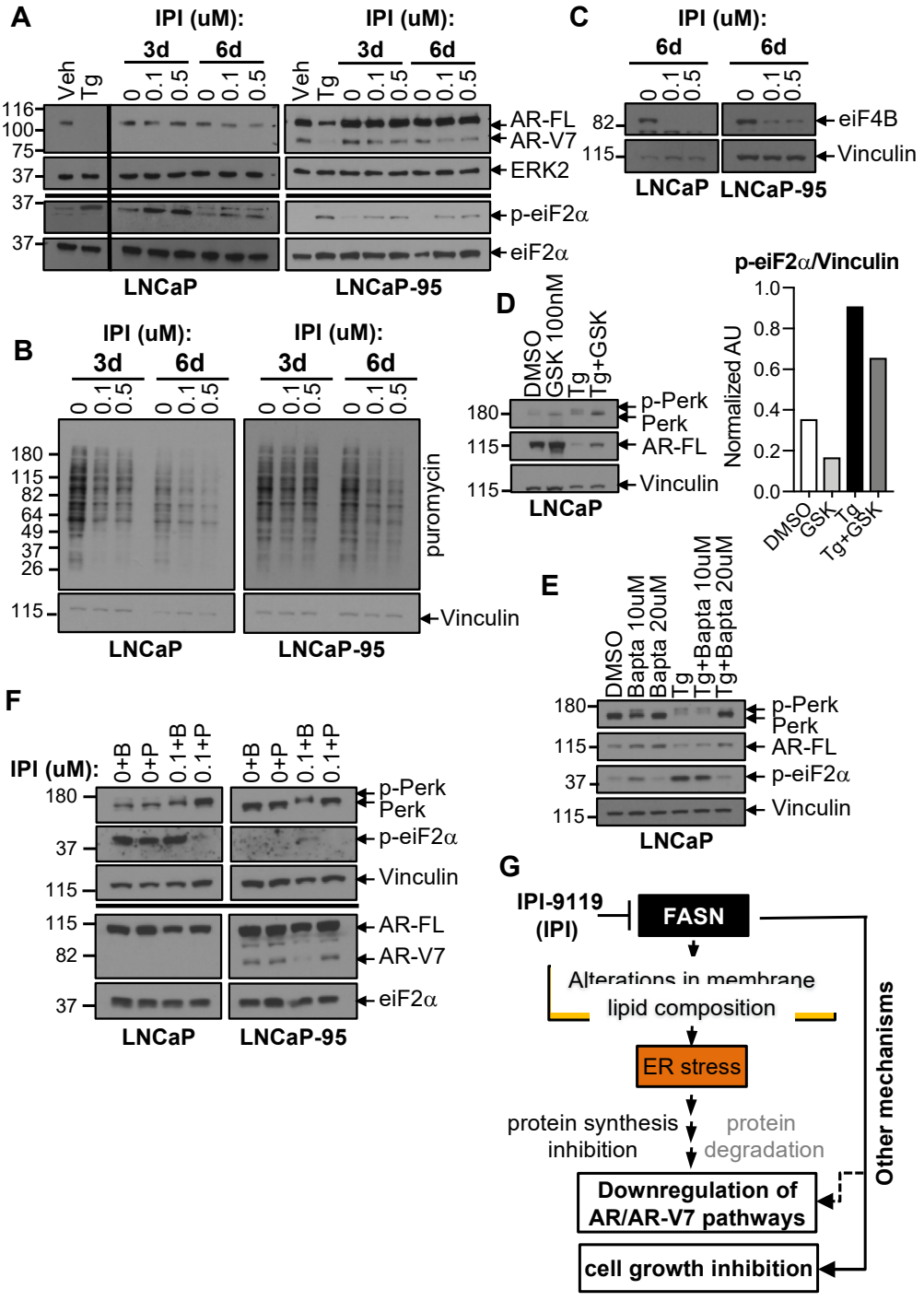

Figure 7. IPI-9119 induces ER stress response and protein translation inhibition.
(**A**) Immunoblotting showing the induction of ER stress marker p-eiF2α in LNCaP and LNCaP-95 cells treated with IPI for 3 and 6 days; (**B**) Immunoblotting with the anti-puromycin antibody (SUnSET assay) showing the reduction of protein synthesis in LNCaP and LNCaP-95 cells treated with IPI-9119 (IPI) for 3 and 6 days; (**C**) Representative immunoblotting showing the downregulation of translation initiator co-factor eiF4B, following treatment with IPI for 6 days. Experiment was repeated twice (LNCaP) and 4 times (LNCaP-95) with similar results. (**D**) (E) Representative immunoblotting showing the rescue of AR expression, following reduction of ER stress using the Ca^{2+} chelant Bapta. (**F**) Representative immunoblotting showing concomitant rescue of IPI-9119-mediated AR/AR-V7 reduction and ER stress, following incubation with Palmitate for 3 days. Palmitate (50 μM) was complexed with BSA (molar ratio 6:1) while control cells were treated with BSA only. (**G**) Schematic representation of the involvement of ER stress in mediating IPI-9119 effects.

Site of performance: Dana-Farber Cancer Institute, University of Minnesota, Twin Cities

DFCI site team: Massimo Loda (PI), Giorgia Zadra (Co-investigator), Leigh Ellis (Co-investigator), Caroline F. Ribeiro (Post-doctoral fellow).
U of M site team: Scott Dehm (co-PI), Yeung Louisa Ho (Post-doctoral fellow), Yingming Li (Research Associate)

5. IPI-9119 Inhibits AR-FL and AR-V7 transcriptional activity.

Analysis of RNA-seq data from LNCaP cells treated with IPI-9119 revealed reduced expression of canonical AR-FL target genes (e.g. KLK3, TMRSS2, NKX3-1) (**Figure 8A**). Accordingly, activity of an AR-responsive luciferase reporter was inhibited by IPI-9119 in LNCaP cells (**Figure 8B**). We also observed suppression of an M-phase cell cycle gene signature previously found to be associated with AR-V7 transcriptional activity [28], but also representing biphasic AR-FL targets (**Figure 8C**) [7]. Significantly, this signature was completely restored by the addition of exogenous palmitate (**Figure 8D)**. More importantly, IPI-9119 inhibited a gene signature found in CRPC bone metastases, which express high mRNA levels of AR-V7 [29] (**Figure 8E**). Similar results were obtained in 22Rv1 (data not shown). Finally, we observed a trending downregulation of a recently published AR-V7-modulated gene set (33 up-regulated genes in common between LNCaP-95 and 22Rv1 cells) identified during analyses of AR-V7-regulated transcriptome and cistrome [30] (**Figure 8F)**. c-MYC, an oncogene commonly amplified in CRPC, had been previously described as an androgen-independent, AR-dependent target gene.). c-MYC protein was significantly reduced in IPI-9119-treated AD and AI cells and rescued by exogenous palmitate (**Figs. 8G**). Pre-ranked GSEA also confirmed the downregulation of a c-MYC transcriptional signature (V1) (**Figure 8H**). Finally, we went back to our findings of IPI-9119-mediated reduction of AR-V7 protein, and its transcriptional activity in CRPC cells to test the combination of IPI-9119 and Enza in 22Rv1, a cell line resistant to Enza and driven by AR-V7. Our data show that the combination of IPI-9119 and Enza was more effective in reducing 22Rv1 cell growth than either of the single agents (**Figure 8I**).

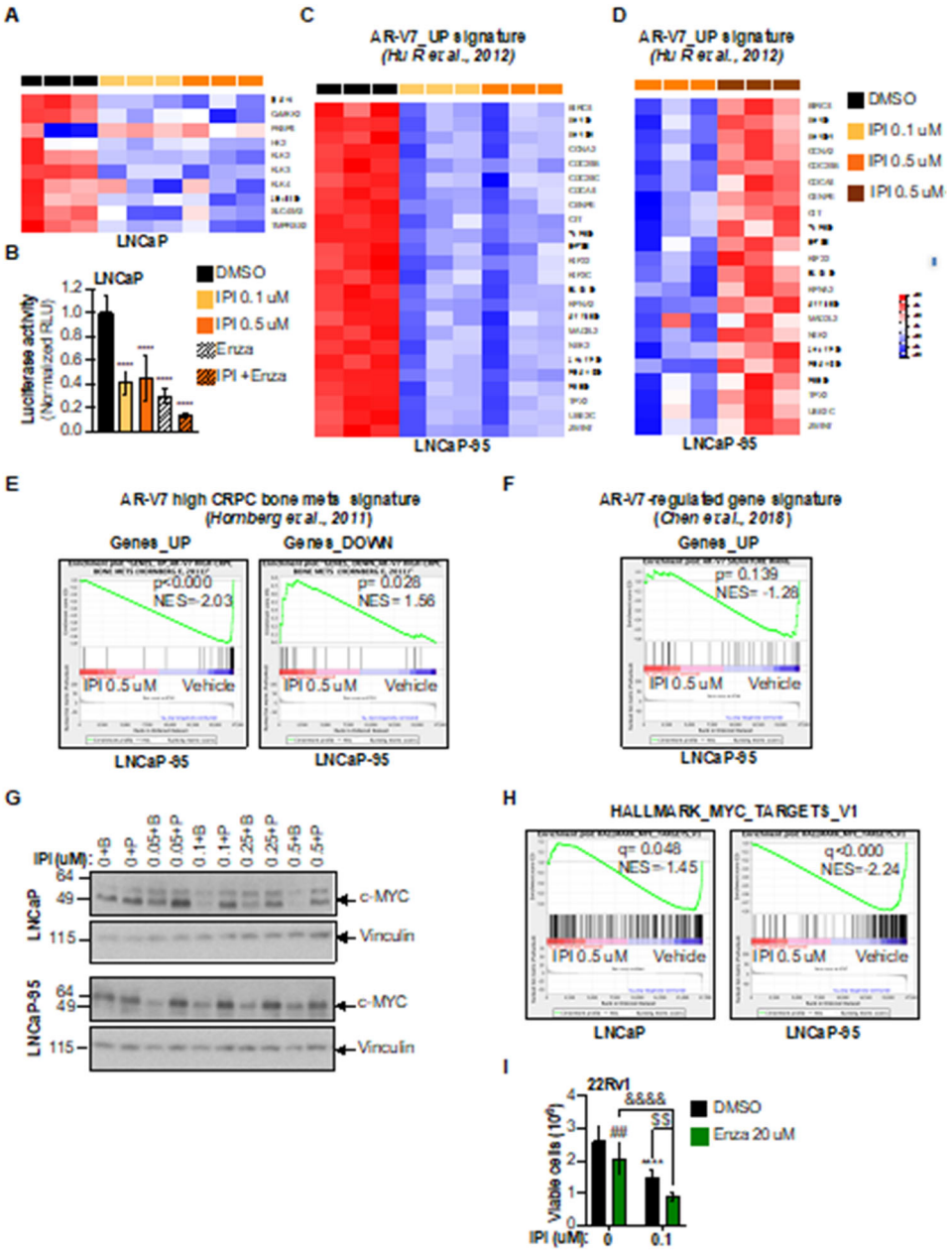

Figure 8. IPI-9119 inhibits AR transcriptional activity and enhances enzalutamide efficacy.
(**A**) Heatmap of canonical AR target genes, following treatment with IPI-9119 (IPI) or DMSO for 6 days. Normalized counts (n=3) are shown. (**B**) Luciferase activity in LNCaP cells treated with IPI for 6 days. ****p<0.0001, one-way ANOVA, followed by Tukey's post hoc test. Data represent mean ± SD (n=3). (**C**) Heatmap of RNA-seq data showing IPI-mediated abrogation of the AR-V7_UP gene signature after 6 days of treatment. Normalized counts are shown (n=3). (**D**) Heatmap of TaqMan™ Array Microfluidic Cards data showing palmitate rescue of the AR-V7_UP gene signature. Results are expressed as fold change of DMSO treatment. Normalized values are shown (n=3). (**E**) Pre-ranked GSEA analysis showing IPI-mediated reversion of a gene signature associated with CRPC bone mets expressing high levels of AR-V7; p-values are indicated. (**F**) Representative immunoblotting showing the reduction of c-MYC protein expression under treatment with IPI for 6 days. Co-incubation with palmitate restored c-MYC expression. Palmitate (50 µM) was complexed with BSA (molar ratio 6:1) while control cells were treated with BSA only. (**G**) Pre-ranked GSEA analysis showing IPI-mediated negative modulation of MYC_TARGETs_V1 signature (Hallmarks; h.all.v5.2s symbols.gmt); FDR values are indicated. (**H**) Cell growth after 6 days of Enza and IPI co-treatment. ****p<0.0001 IPI *vs* DMSO, $^{\#\#}$p<0.01 Enza *vs* DMSO, $^{\$\$}$p<0.01 IPI+Enza *vs* IPI, $^{\&\&\&\&}$p<0.01 IPI+Enza *vs* Enza, two-way ANOVA followed by Sidak's post hoc test.

Site of performance: Dana-Farber Cancer Institute, University of Minnesota, Twin Cities
DFCI site team: Massimo Loda (PI), Giorgia Zadra (Co-investigator), Leigh Ellis (Co-investigator), Caroline F. Ribeiro (Post-doctoral fellow).
U of M site team: Scott Dehm (co-PI), Yeung Louisa Ho (Post-doctoral fellow), Yingming Li (Research Associate)

6. In human mCRPC cases FASN protein is co-expressed with AR-FL and AR-V7

Analysis of human tissue from metastatic sites related to advanced prostate cancer show co-expression of AR-FL and AR-V7 with FASN. Tissue microarrays (TMAs) from 55 mCRPC patients, excluding neuroendocrine cases, were used for this analysis. In 87% of all metastases there was a significant association with FASN and AR-FL expression. AR-V7 positivity concomitant to FASN expression was observed in 39% of bone metastases, and 12% of visceral sites (**Figure 9A, B, D**). This indicates that FASN may be targeted in the majority of mCRPC, independently of AR-V7 status. Twenty-two of the cases analyzed were resistant to Enzalutamide and/or Abiraterone, and within this subset 77% of cases were positive for FASN and AR-V7. In addition, AR-V7 was detected in up to 25% of Enza/Abi treatment-naïve cases, always co-expressed with FASN (**Figure 9C**).
These findings have important therapeutic implications, particularly in the castration-resistant setting, since most human CRPC metastases we examined co-expressed FASN and AR-FL. Inhibition of de-novo lipogenesis could be proposed in association with Enza and/or Abi or taxanes, to delay/overcome resistance. Alternatively, FASN inhibition could be undertaken in tumors that are still AR-driven once resistance has emerged. Carefully designed clinical trials are required to establish the therapeutic timing, combinatorial regimens and the population suitable for treatment with FASN inhibitors.

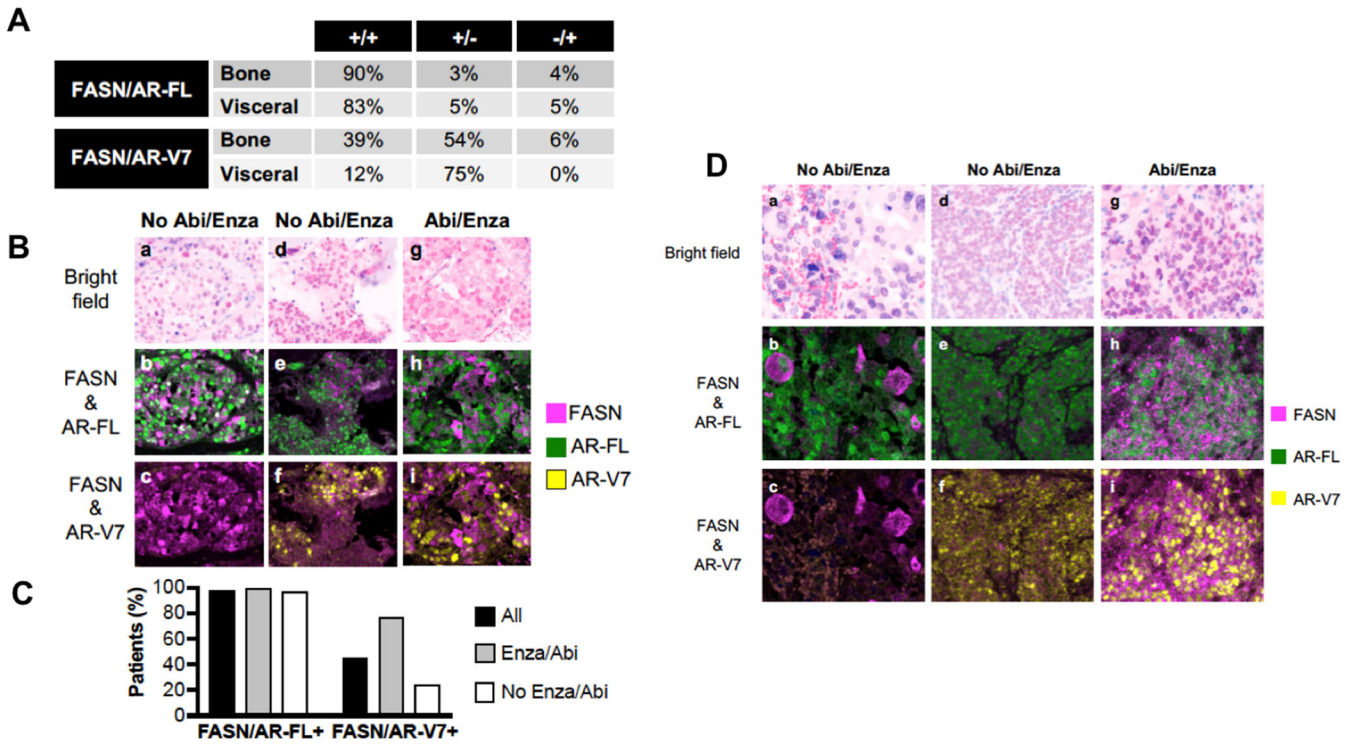

Figure 9. FASN is co-expressed with AR-FL and AR-V7 in human mCRPCs.
(**A**) Status of FASN, AR-FL, AR-V7 in metastatic sites. Data are expressed as a percentage of either osseous or visceral metastases. (**B**) Representative images of FASN co-expression with AR-FL and AR-V7 (20X) in bone metastases: Bright field (a), FASN/AR-FL staining (b), FASN/AR-V7 staining in AR-V7-negative bone metastasis from a mCRPC Enza/Abi-naïve patient (c); Bright field (d), FASN/AR-FL staining (e), FASN/AR-V7 staining in AR-V7-positive bone metastasis from a mCRPC Enza/Abi-naïve patient (f); Bright field (g), FASN/AR-FL staining (h), FASN/AR-V7 staining in AR-V7-positive bone metastasis from a mCRPC Enza/Abi-treated patient (i). (**C**) Bar graph showing the percentage of patients with FASN/AR-FL and FASN/AR-V7 co-expression in all mCRPC patients analyzed or in the subset treated with Enza/Abi. (**D**) Representative images of FASN co-expression with AR-FL and AR-V7 (20X) in liver metastases: Bright field (a), FASN/AR-FL staining (b), FASN/ AR-V7 staining in AR-V7-negative liver metastasis from a mCRPC Enza/Abi-naïve patient (c); Bright field (d), FASN/AR-FL staining (e), FASN/ AR-V7 staining in ARV7-positive liver metastasis from a mCRPC Enza/Abi-naïve patient (f); Bright field (g), FASN/AR-FL staining (h), FASN/AR-V7 staining in AR-V7-positive liver metastasis from a mCRPC Enza/Abi-treated patient (i)

Site of performance: Dana-Farber Cancer Institute

DFCI site team: Massimo Loda (PI), Giorgia Zadra (Co-investigator), Caroline F. Ribeiro (Post-Doctoral fellow).

7. FASN inhibition induces AR and AR-V7 specific degradation through proteasome

As proposed in **Aim 3** and **SOW for years 2 and 3**, we investigated the mechanism of AR signaling downregulation after IPI-9119 treatment. To confirm that FASN inhibition induces AR and AR-V7 protein degradation, we combined IPI-9119 treatment with MG132, a potent proteasome inhibitor. In LNCaP cell lines, it's observed that inhibition of proteasome leads to increased AR-FL levels in comparison to IPI-9119 treatment alone, for both 0.1 and 0.5uM conditions **(Figure 10A).** In LNCaP-95 cells, AR-V7 expression levels are also increased with MG132 treatment in comparison to IPI-9119 alone, while AR-FL levels do not seem to significantly differ in the presence or absence of proteasome inhibitor **(Figure 10B).** To confirm FASN inhibition-driven AR-V7 downregulation mainly regulated at the protein level we treated LNCaP cells stably overexpressing AR-V7 under the inducible TRE3G promoter with IPI-9119; ectopic AR-V7 protein expression was significantly reduced by IPI-9119 treatment **(Figure 10C).** Interestingly, when we express AR-V7 similarly in the AR-null cell line PC3 no reduction is observed following IPI-9119 treatment for 6 days, indicating a degradation mechanism that involves receptor dimerization **(Figure 10D).**

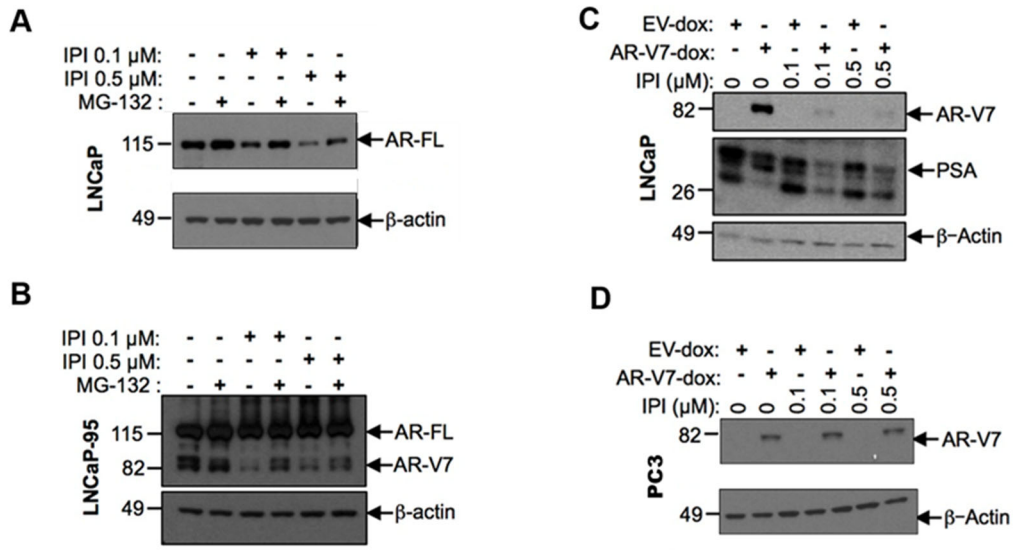

Figure 10. IPI-9119 induces AR and AR-V7 proteasome degradation.

A) Representative immunoblotting of AR-FL expression in LNCaP cells following treatment with IPI-9119 at 0.1 uM and 0.5uM for 6 days and with the proteasome inhibitor MG132 at 20uM for 4h. **B)** Representative immunoblotting of AR-FL and AR-V7 expression in LNCaP-95 cells following treatment with IPI-9119 at 0.1 uM and 0.5uM for 6 days and with the proteasome inhibitor MG132 at 20uM for 4h. **C)** Representative immunoblotting of PSA and AR-V7 overexpression with inducible agent doxycycline in LNCaP cells following treatment with IPI-9119 at 0.1 uM and 0.5uM for 6 days. **D)** Representative immunoblotting of AR-V7 overexpression with inducible agent doxycycline in AR-null cells PC3 following treatment with IPI-9119 at 0.1 uM and 0.5uM for 6 days.

Site of performance: Weill Cornell Medical College
WCM site team: Massimo Loda (PI), Caroline F. Ribeiro (Research associate).

8. FASN inhibition enhances Enzalutamide efficacy in reducing cell growth

As proposed in **Aim 1** and **SOW for years 2 and 3**, we investigated the therapeutic efficacy of combining the FASN inhibitor IPI-9119 with the androgen receptor antagonist Enzalutamide. In our previous report we show that in prostate cancer cell line 22Rv1 the combinatorial treatment enhances cell growth reduction in comparison to IPI-9119 and Enzalutamide alone. Now, we confirmed these findings in 3D organoid models derived from human CRPC (MSK-PCa3). As shown in **Figure 11A** organoids growth, as measure by diameter size, is reduced when Enzalutamide and IPI-9119 are combined, at higher efficacy than either agent alone. Cell growth, as

measured by number of viable cells, is also increased in the combinatorial treatment (**Figure 11B).** Altogether, this data show that FASN inhibition potentiates Enzalutamide therapeutic efficacy in pre-clinical models and can be an option to overcome treatment resistance in advanced prostate cancer.

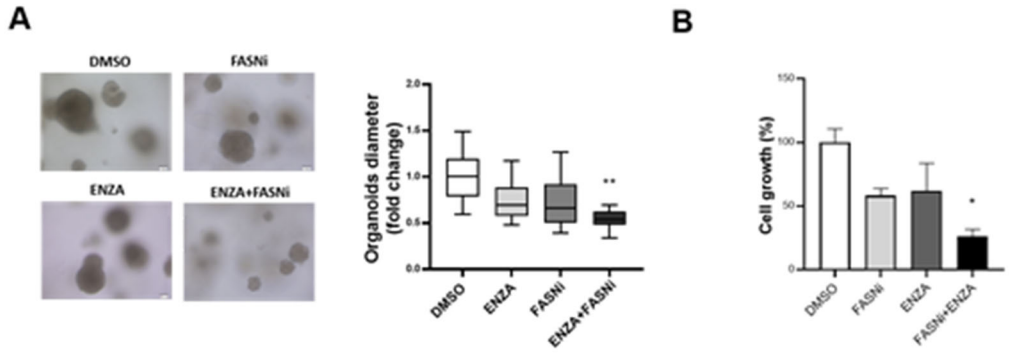

Figure 11. **IPI-9119 enhances enzalutamide efficacy in human organoid model of CRPC**
A) Growth of 3D organoid models of human CRPC after 25 days treatment with IPI-9119 at 0.5uM and Enzalutamide at 20uM. Data are expressed as organoid diameter fold change in comparison to the control DMSO. **p<0.01, Anova and Tukey's test. **B)** Cell growth of CRPC organoid models after FASN inhibition determined through trypan blue exclusion method in automated cell counter (Vi-Cell BLU). Data expressed as mean number of viable cells ± SD and plotted as % DMSO. *p<0.05, Anova and Tukey's test.

Site of performance: Weill Cornell Medical College
WCM site team: Massimo Loda (PI), Caroline F. Ribeiro (Research associate).

9. FASN inhibition modulates DNA damage repair and sensitizes CRPC cells and organoid models to PARP inhibitor

As proposed in our previous progress report, we decided to investigate how FASN inhibition could be combined with other therapies to potentiate anti-tumoral effect. Pre-ranked GSEA showed that FASN inhibition down-regulates gene signatures associated with DNA damage response: DNA repair, double strand break repair and Homologous Recombination (**Figure 12A)**. At the protein level, we observed that phosphorylation of H2A histone family member X is increased following IPI-9119 treatment, a known marker of double-strand breaks in dsDNA

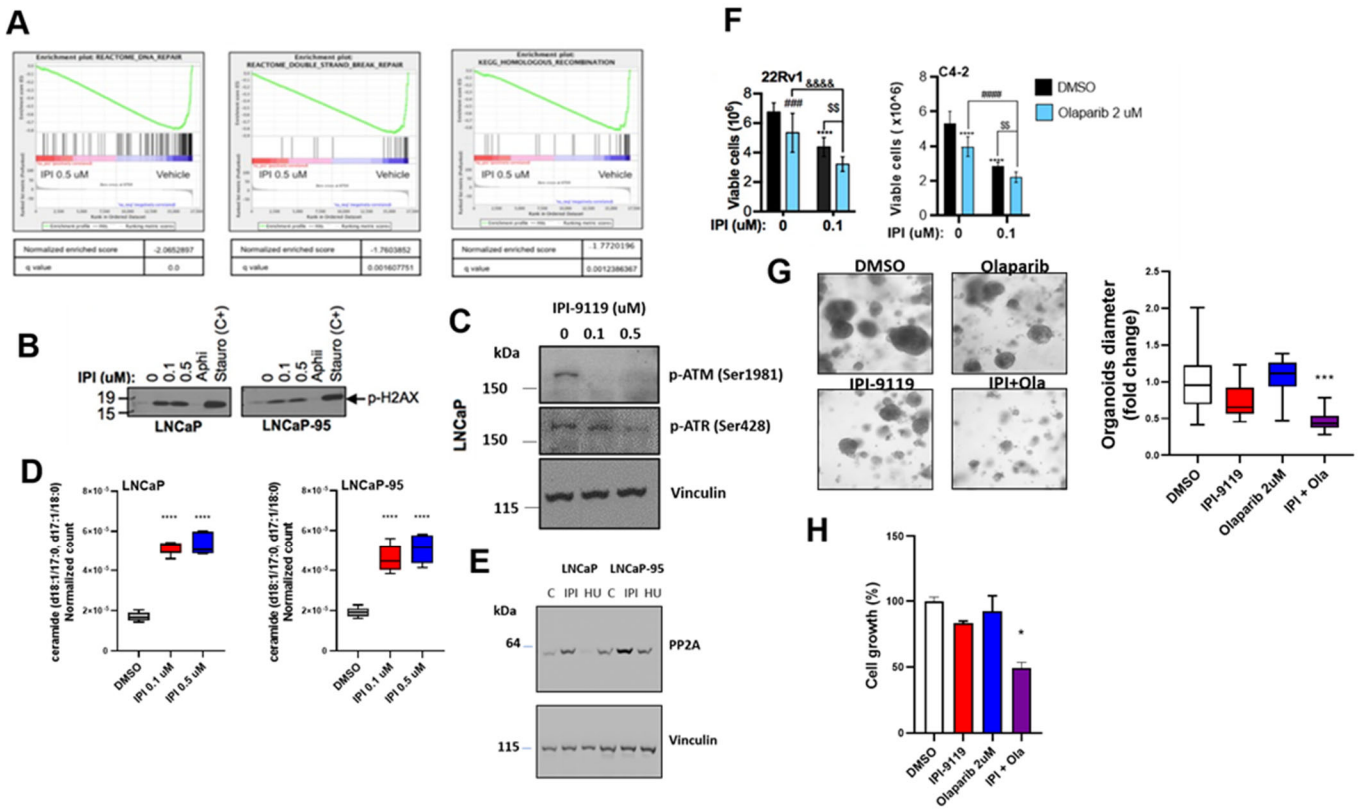

Figure 12. IPI-9119 inhibits DNA damage response, induces ceramide accumulation and enhances Olaparib efficacy. **A)** Pre-ranked GSEA analysis showing IPI-mediated downregulation of three gene signatures associated with DNA damage response: DNA repair, double strand break repair and Homologous Recombination; FDR-values are indicated. **B)** Representative immunoblotting showing increased phosphorylation of histone H2ax after IPI-9119 treatment at 0.1 and 0.5uM for 6 days in both LNCaP and LNCaP-95 cells. The S-phase inhibitor aphidicolin (Aphi, 0.3 µg/mL, 3 h) and the apoptosis inducer staurosporine (Stauro, 1 µM for 24 h) were used as controls. **C)** Representative immunoblotting showing decreased phosphorylation of ATM and ATR after FASN inhibition with 0.1 and 0.5uM of IPI-9119 for 6 days in LNCaP cells. **D)** Box plots showing the levels of ceramide from metabolomics data, (n = 6 per condition). ****q < 0.0001, Anova and Tukey's test. **E)** Representative immunoblotting showing increased PP2A phosphatse levels after FASN inhibition with IPI-9119 treatment at 0.1 uM for 6 days in both LNCaP and LNCaP-95 cells. The DNA damage response inducer hydroxyurea (2mM for 4h) was used as control. **F)** Cell growth of C4-2 and 22Rv1 cells after 6 days of Olaparib 2uM and IPI-9119 0.1uM co-treatment. Data expressed as mean number of viable cells ± SD and plotted as % DMSO. ****p<0.0001 IPI vs DMSO, ###p<0.01 Ola vs DMSO, $$p<0.01 IPI+Ola vs IPI, &&&&p<0.01 IPI+Ola vs Ola, two-way ANOVA followed by Sidak's post hoc test. **G)** Growth of 3D organoid models of human CRPC after 25 days treatment with IPI-9119 at 0.5uM and Olaparib at 2uM. Data are expressed as organoid diameter fold change in comparison to the control DMSO. ***p<0.001, Anova and Tukey's test. **H)** Cell growth of CRPC organoid models after FASN inhibition determined through trypan blue exclusion method in automated cell counter (Vi-Cell BLU). Data expressed as mean number of viable cells ± SD and plotted as % DMSO. *p<0.05, Anova and Tukey's test.

(**Figure 12B),** while phosphorylation of Ataxia-telangiectasia mutated (ATM) kinase and Ataxia-telangiectasia and Rad3-related protein (ATR) is reduced, showing impairment of DNA damage repair pathways (**Figure 12C).** Ceramides, sphingolipids with important role in the cellular metabolism, have been implicated with PP2A activation; untargeted MS-based metabolomics shows that IPI-9119 treatment increases ceramide accumulation in prostate cancer cells (**Figure 12D)** concomitantly to increased PP2A expression (**Figure 12E**). Due to the significant modulation of DNA damage response in prostate cells with FASN inhibition, we decided to evaluate if IPI-9119 could potentiate therapeutic efficacy of the PARP inhibitor Olaparib. Combination treatment of IPI-9119 with Olaparib showed increased reduction of cell growth *in vitro* in CRPC cell lines (**Figure 12F).** Organoid models of CRPC also show reduced size **(Figure 12G)** and cell viability **(Figure 12H)** when co-treated with the FASN inhibitor and PARP inhibitor. Altogether, this data shows that FASN has a role in DNA damage response and BRCA1/2 non-mutated tumors could benefit from FASN inhibition to target Homologous Recombination and sensitize cells to Olaparib, increasing therapeutic options for prostate cancer patients.

Site of performance: Weill Cornell Medical College
WCM site team: Massimo Loda (PI), Caroline F. Ribeiro (Research associate).

10. Lipidome remodeling in prostate cancer cells following FASN inhibition

We have previously shown that ER stress is involved in inducing AR pathway downregulation as well as mediating the anti-cancer effect of FASN inhibition. Membrane lipid perturbation has been demonstrated to be involved in ER stress[24]. We hypothesized that IPI-mediated FASN inhibition caused alterations in membrane lipid composition which in turn induce ER stress. Therefore, to reveal the lipid metabolic effects induced by IPI-9119, we used an ESI-MS based mass spectrometry-based comprehensive lipidomic profiling approaches to examine over 1800 lipid species across 17 different lipid classes in AR-positive LNCaP and AR/AR-variant positive LNCaP95 prostate cancer cell lines. Cells were treated with 500nM IPI-9119 and collected at day 1, 3, and 6 for lipidomic analysis. We focused on the most abundant lipid species which we defined as those representing more than 2% of their total lipid class in data analysis.

To validate the function of IPI-9119 in inhibiting FASN activity, we first examined the lipidomic changes of triacylglycerides (TAGs). As illustrated in **Figure 13A**, FASN catalyzes the synthesis of palmitate from malonyl-CoA and acetyl-CoA. IPI-9119 treatment induced a progressive decrease in the levels of abundant TAG species as measured by the log2 fold change in IPI-9119-treated cells over vehicle treated cells (**Figure 13B;** TAG species nomenclature indicates the total number of fatty acid carbons : the total number of double bonds / the total number of fatty acid carbons in the sn-1 position acyl chain : the total number of double bonds in the sn-1 position acyl chain). These data validated the effects of IPI-9119 in inhibition of fatty acid *de novo* synthesis in our models.

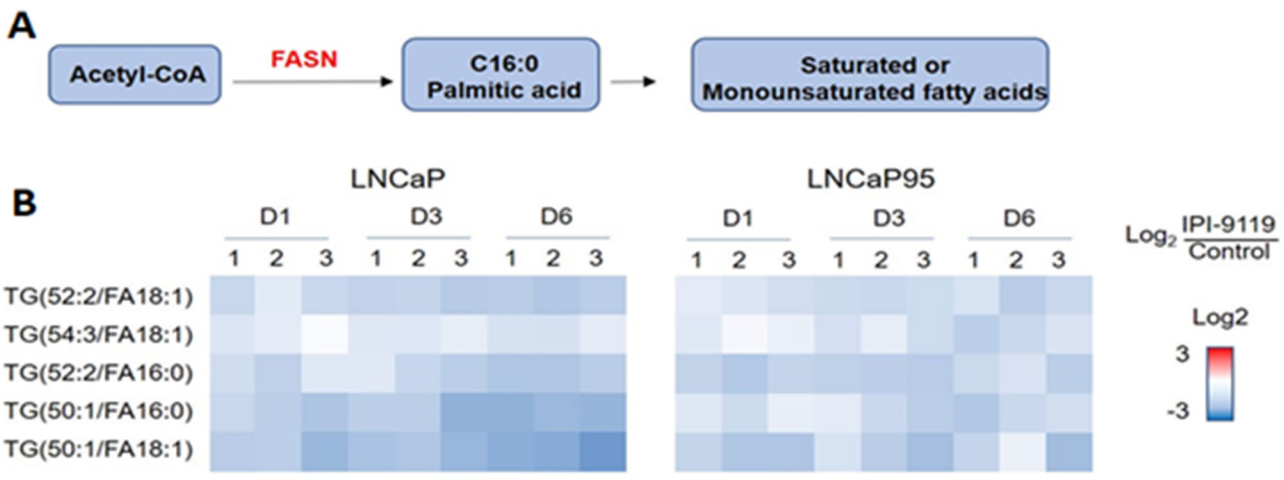

Figure 13. IPI-9119 induces a progressive decrease in the levels of abundant triacylglyceride (TAG) species in prostate cancer cell lines.
A) The *de novo* synthesis of fatty acids. The key enzyme, FA synthase (FASN), catalyzes the synthesis of palmitate from malonyl-CoA and acetyl-CoA. **B)** Heatmap of log2 ratios of the levels of the most abundant TAG species in IPI-9119-treated cells over vehicle treated cells (n=3).

We then focused on the two major membrane lipid species, sphingolipids (SLs) and glycerophospholipids (GPLs). As illustrated in **Figure 14A**, SLs consist of a sphingosine base (the backbone of SLs), an N-acyl chain and a head group. Hydroxylation and unsaturation determine the sphingosine base type whereas the head group defines the sphingolipid name. *De novo* synthesis of SL is illustrated in **Figure 14B.** Ceramide is the building block of all SLs and ceramide synthase (CERS) is the key regulator in N-acylation of sphinganine to dihydroceramide (DHCer) which is subsequently reduced to ceramide. Head groups are added to ceramide to make complex SLs, such as sphingomyelin (SM), glycosylceramide (GlcCer), etc. To link the lipid metabolic changes and expression of AR and AR variants, we selected specific lipid species which increased with the same kinetics as the reduction in expression of AR and AR variants in IPI time-dependently simultaneously in both LNCaP and LNCaP95 cells.

As shown in **Figure 14C**, IPI-9119 promoted a progressive increase in Cer(d18:1/22:4), Cer (d18:1/24:0) and Cer [d181:1/20:4; for this nomenclature, the sphingoid bases are indicated by the number of hydroxyl groups (d denotes two) and the chain length (typically 18 carbons) : the number of double bonds / the acyl chains length : the number of double bonds]. Ceramide levels were determined by the Log2 fold change in IPI-treated cells over vehicle treated cells. Moreover, the levels of specific sphingomyelin species SM(d18:1/24:0) and SM(d18:1/22:0) were also increased progressively from day 1 to day 6 following IPI-9119 treatment (**Figure 14D)**. These

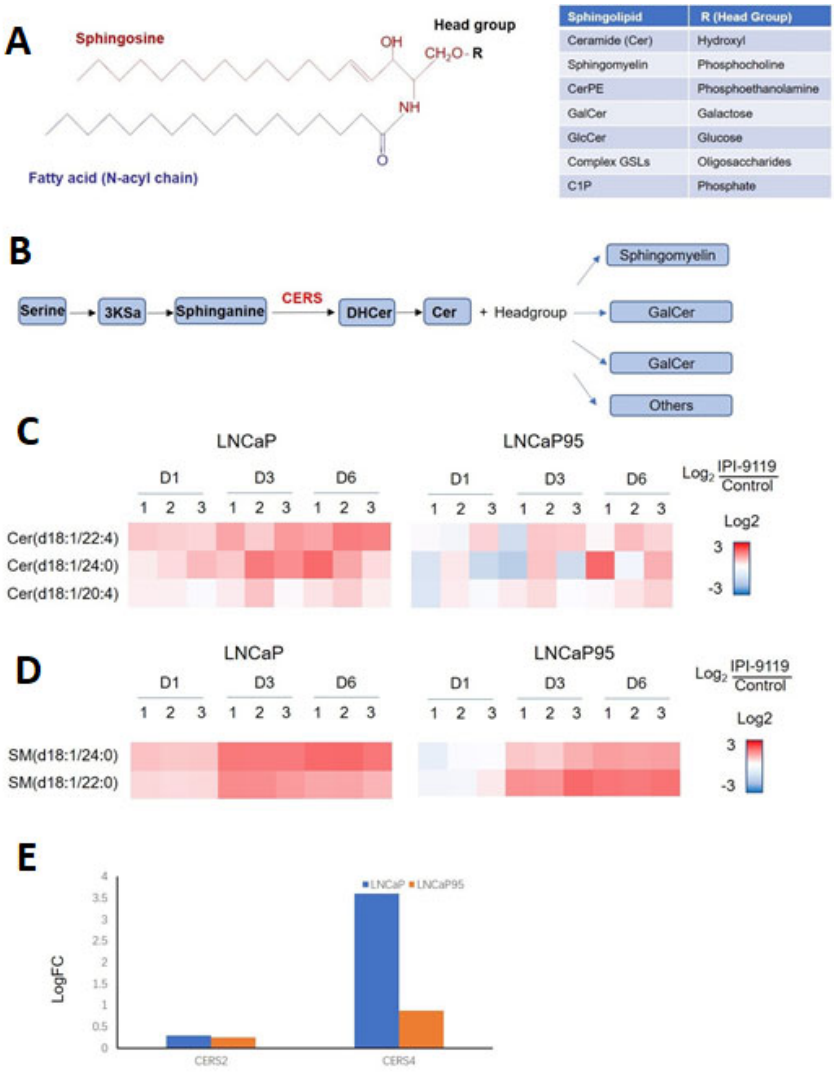

Figure 14. IPI-9119 promotes a progressive increase in specific membrane sphingolipid species and concomitant upregulation of gene expression of relevant enzymes regulators in prostate cancer cell lines.
A) Structure of membrane sphingolipids. **B)** Synthesis pathway and head group modification of sphingolipid species. CERS: ceramide synthases. **C)** Heatmap of log2 ratios of the abundance of ceramide species in IPI-9119-treated cells over vehicle treated cells (n=3). **D)** Heatmap of log2 ratios of the abundance of sphingomyelin species in IPI-9119-treated cells over vehicle treated cells (n=3). **E)** Bar plot log2 ratios of gene expression of specific ceramide synthase in IPI-9119-treated cells over vehicle-treated cells (n=3).

sphingolipids vary mainly in the length of their acyl chains which are regulated by specific CERS. Each CERS displays specificity toward fatty acyl CoA of defined chain length. Therefore, we decided to examine the gene expression profiles of CERS in both LNCaP and LNCaP95 cells which were treated by 500nM IPI-9119 for 6 days. As shown in **Figure 14E,** RNA-seq gene expression profiling showed that CERS2 and CERS4 were upregulated in both cells following IPI treatment. CERS2 has specificity toward acyl chains with the length of carbon 22 to 24 while CERS4 mainly targets those with the length of carbon 18-22[31]. These results are consistent with the progressive increase in the levels of the specific ceramides and sphingomyelins (**Figure 14D, Figure 12D)**. Altogether, these results indicate that IPI-mediated FASN inhibition induced progressive increases in the levels of specific sphingolipid species accompanied by the concomitant upregulation of the key regulators in

sphingolipid synthesis. The kinetics of these changes is consistent with the kinetics of the decrease in expression levels of AR and AR variants as well as the induction of ER stress in IPI-treated cells[32].

We next examined the changes in GPLs following IPI-9119 treatment. As illustrated in **Figure 15A**, GPLs consist of a glycerol backbone, two fatty acid chains at the *sn*-1 and *sn*-2 positions, a phosphatidyl ester attached to the terminal carbon and a head group linked to the phosphatidyl ester. The head groups define the name of specific GPL species. De novo synthesis of GPLs is illustrated in **Figure 15B.** When free fatty acids are incorporated in GPLs, the activation of fatty acids by CoA is required. Acyl-CoA synthetases (ACSs) are the key regulators of this process[33]. Another critical regulation step in GPL synthesis is the conversion of lysophosphatidic acid (LPA) to phosphatidic acid (PA) by Acylglycerophosphate acyltransferases (AGPATs). As shown in **Figure 15C,D**, IPI-9119 promoted a progressive increase in the level of PC (16:1/18:1), PI (18:0/18:1) and PI (16:1/18:0) in both cells (GPL nomenclature indicates the chain length of the sn-1 fatty acid chain:number

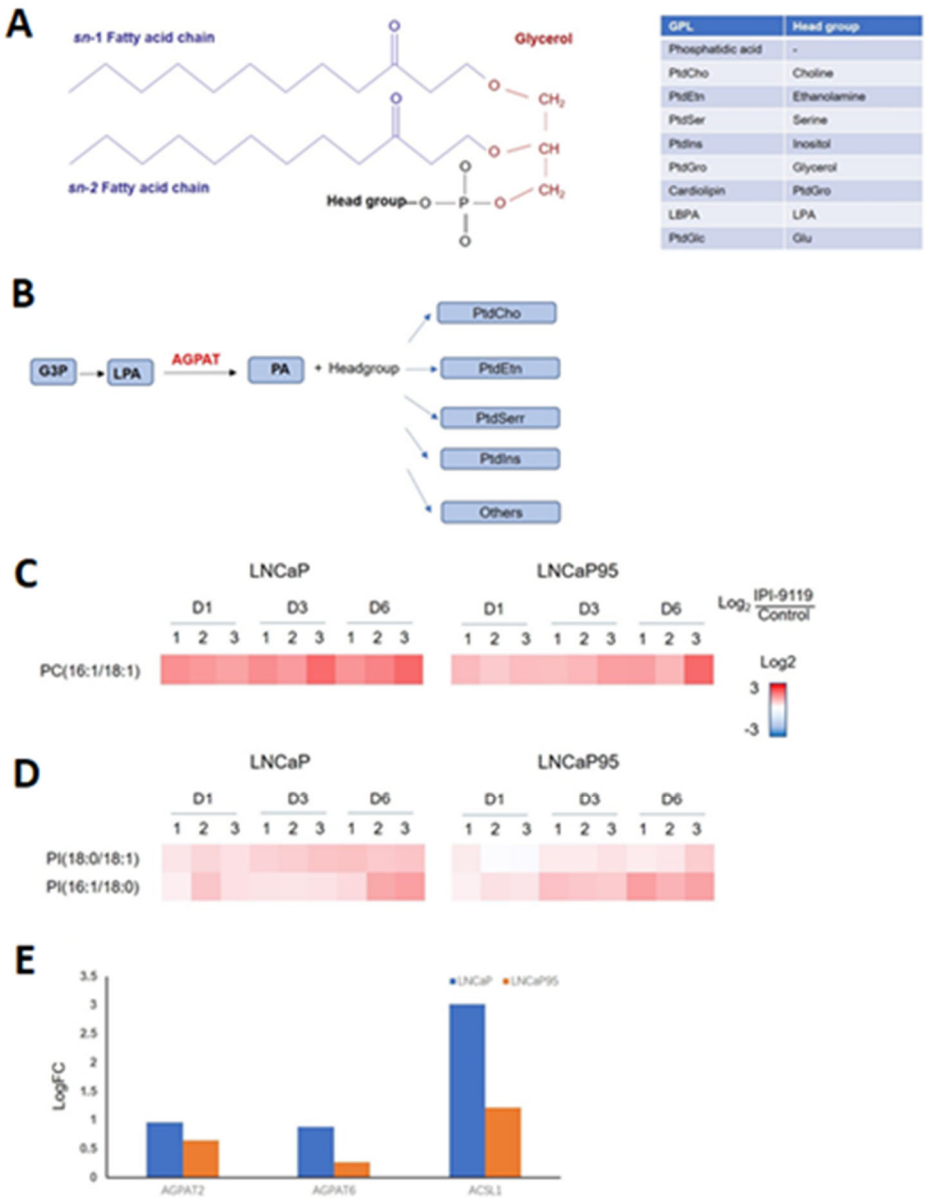

Figure 15. IPI-9119 leads to a progressive increase in specific membrane glycerophospholipid (GPLs) species and concomitant upregulation of gene expression of relevant enzymes regulators in prostate cancer cell lines.
A) Structure of GPLs. **B)** Synthesis pathway and head group modification of GPL species. AGPAT: 1-acylglycerol-3-phosphate O-acyl-transferases. **C)** Heatmap of log2 ratios of the abundance of PtdCho in IPI-9119-treated cells over vehicle treated cells (n=3). **D)** Heatmap of log2 ratios of the abundance of PtdIn IPI-9119-treated cells over vehicle treated cells (n=3). **E)** Bar plot of log2 ratios of gene expression of ACSL1, AGPAT2 and AGPAT6 in IPI-9119-treated cells over vehicle-treated cells (n=3).

of double bonds in the sn-1 fatty acid chain / the chain length of the sn-2 fatty acid chain:number of double bonds

in the sn-2 fatty acid chain). Similarly, we examined the gene expression profiles of the regulators of GPL metabolism in both LNCaP and LNCaP95 cells treated with 500nM IPI-9119 for 6 days. As shown in **Figure 15E,** RNA-seq gene expression profiling showed that ACSL1, AGPAT2 and AGPAT6 were upregulated in both cell lines following 6 days IPI treatment. These results are consistent with the progressive increase in the levels of the specific GPLs in **Figure 15C,D**. Altogether, these results indicated that IPI-9119 mediated FASN inhibition induced progressive increases in the levels of specific GPL species accompanied by the concomitant upregulation of key regulators in GPL synthesis. Moreover, the kinetics of these changes were consistent with the kinetics of the decrease in expression of AR-FL and AR-V7 as well as the induction of ER stress in IPI-treated cells[32].

Collectively, these data revealed widespread changes in lipid metabolites and expression of genes that regulated lipid metabolism. Our work demonstrates upregulation of SL and GPL species with kinetics that mirror the reduction in expression of AR and AR variants in IPI-treated prostate cancer cells.

Site of performance: University of Minnesota, Twin Cities
University of Minnesota site team: Scott Dehm (PI), Yeung Louisa Ho (Post-doctoral fellow), Yingming Li (Research Associate)

11. Lipidome characterization in PDX models of prostate cancer (LuCaP series)

To better understand the lipidome role in prostate cancer and to identify therapeutic targets, we performed lipid profiling studies in patient-derived xenograft models (PDX). Our data suggest that LuCaP136 and 136CR have higher amounts of monounsaturated fatty acids (MUFAs) than LuCaP35, 35CR, 86.2, and 86.2CR, which reflects higher expression of FADS2 and SCD **(Figure 16A, B),** desaturase enzymes that catalyze unsaturation of fatty acids through the insertion of double bonds between defined carbons of the fatty acyl chain. Interestingly, FADS2 pathway has never been exploited as an alternative to SCD in lipid metabolism of prostate cancer. Since bumped kinase inhibitors (BKI) commonly decrease expression of FADS2 and ELOVL6 transcripts based on our RNAseq data **(Figure 16C)**, we reasoned that effective inhibition of fatty acid synthesis and desaturation can be achieved

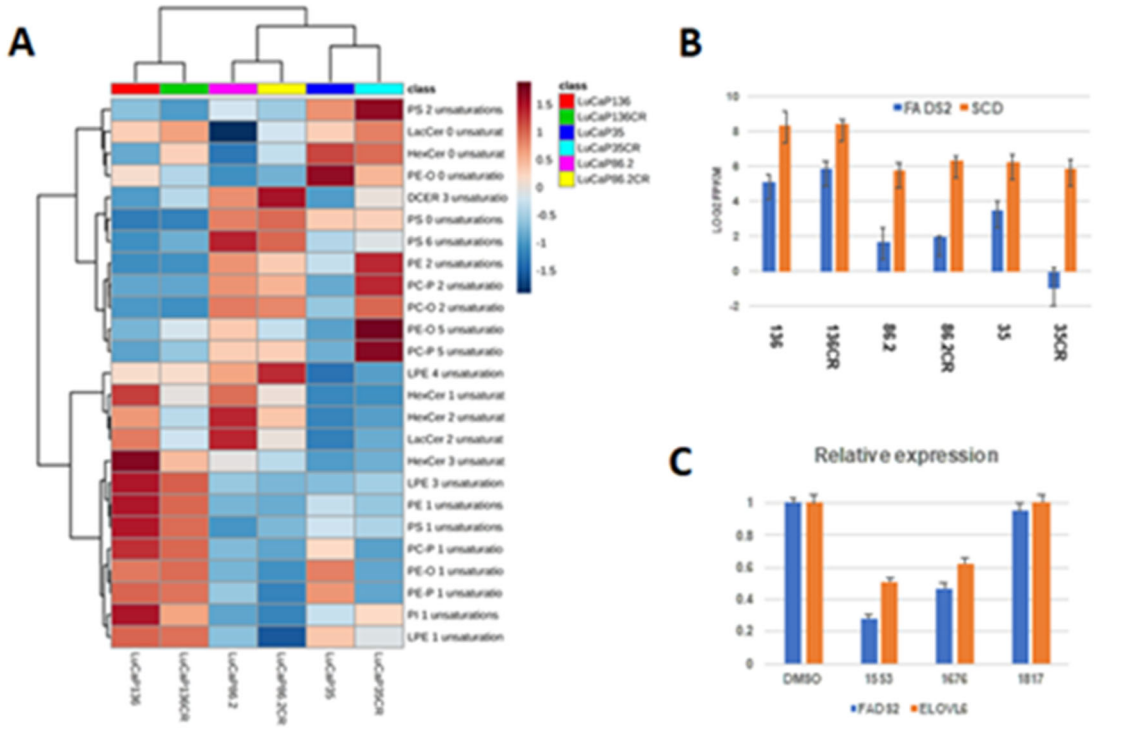

Figure 16. Lipid profiling of PDX models LuCaP series.
A) Lipidomic study of xenograft LuCaP35, 86.2, 136, and their castration resistant (CR) derivates. 136 and 136CR are unique in enrichment of MUFAs e.g. in the form of phosphatidylethanolamine (PE) and phosphatidylserine (PS). **B)** Those properties reflect higher expression of desaturases SCD and FADS2 in 136 tumors than others (RNA-seq based expression prolife). **C)** RNA-seq based expression analysis of ELOVL6 and FADS2 in LNCaP95 treated with BKI 1553 and 1676 and negative control 1817.

by a combination therapy with SCD inhibitor and BKI 1553, a glycolysis inhibitor that we identified as a downregulator of ACC activity. Moreover, FASN substrate malonyl-CoA is produced by ACC, whose phosphorylation at Ser79 inhibits its enzymatic activity and is promoted by inhibition of FASN as well as glycolysis.

Site of performance: University of Washington, Seattle
University of Washington site team: Stephen Plymate (PI), Cynthia Sprenger, Shihua Sun, Kathryn Epilepsia, Soojin Kim, Takuma Uo (research Assistant Professor)

12. Bioenergetics and mitochondrial alterations

The inhibition of palmitate synthesis by IPI-9119 leads to malonyl-carnitine accumulation **(Figure 5C).** As consequence, carnitine palmitoyl transferase (CPT-1) is inhibited and reduces fatty acid oxidation in the mitochondria (FAO). To assess FASN inhibition effect on cell bioenergetics and mitochondria function, we performed Oxygen Consumption and Extracellular Acidification Analysis following IPI-9119 treatment, using the

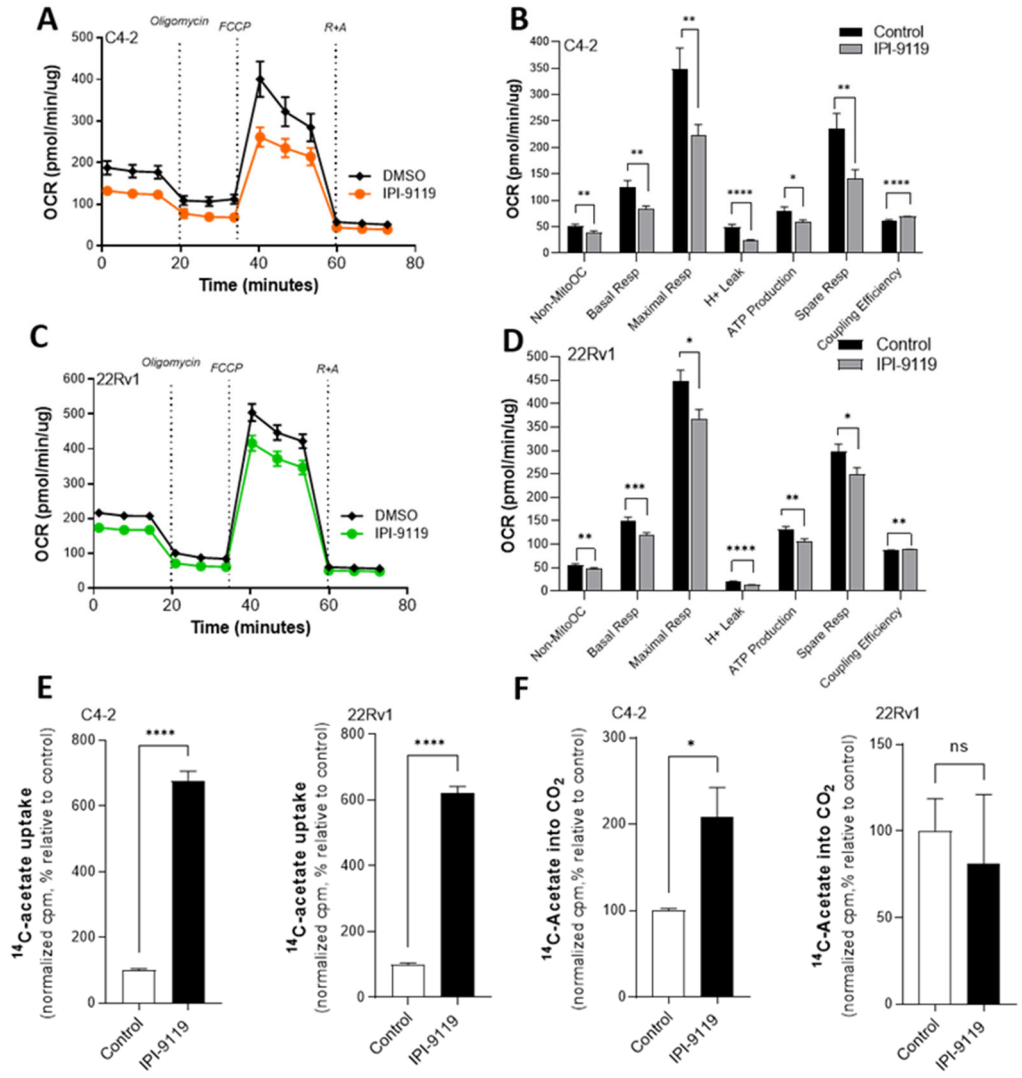

Figure 17. Bioenergetics and energy source in CRPC cells following FASN inhibition by IPI-9119
A,C) oxygen consumption rate (OCR) measured with or without IPI-9119 following serial injections of oligomycin, FCCP, and rotenone/antimycin A in C4-2 and 22Rv1 cells. **B,D)** Quantification of several respiratory parameters in C4-2 and 22Rv1 cells. Results expressed as pmol/min/ug, mean values ± SEM, multiple unpaired t-test with Welch correction, ****p<0.0001, *** p<0.001, ** p<0.01, * p<0.05. **E)** ^{14}C-Acetate uptake assessed in C4-2 and 22Rv1 cells total lysate. Results are expressed as percentage of control, counts per minute (cpm) normalized to viable cells. Mean values ± SD, unpaired t-test, ****p<0.0001. **F)** Acetate oxidation measured by ^{14}C-CO_2 release by cells. Results are expressed as percentage of control, counts per minute (cpm) normalized to viable cells. Mean values ± SEM, unpaired t-test, *p<0.05.

Seahorse XFe96 Analyzer (*Agilent Technologies, Inc*.), in two CRPC cell lines: C4-2, that express only AR-FL, and 22Rv1, that express both AR-FL an AR-V7. FASN inhibition decreased several respiratory parameters, such as basal and maximal respiration, proton leak, ATP-linked respiration and spare respiratory capacity **(Figure 17A-D)**. Interestingly, non-mitochondrial oxygen consumption, the cell capability of respond to changes in energetic demand, is also decreased with IPI-9119 treatment in both cells. To determine how these changes in mitochondrial function alter cell energy source, we evaluated the effect of IPI-9119 in acetate utilization using radiolabeled molecule, and we observed that, for both cell lines, the uptake of acetate is upregulated with FASN inhibition **(Figure 17E)**. Acetate oxidation, however, is only increased with IPI-9119 treatment in C4-2 cells, while 22Rv1 cells do not alter the rate of acetate conversion into CO_2 **(Figure 17F)**.

In line with these findings, we observed that FASN blockade increases mitochondrial superoxide anion levels in both cells, as observed by increased MitoSox oxidation **(Figure 18A)**. The maintenance of mitochondria membrane is fundamental to its function, so we analyzed several lipid classes through LC-ESI/MS/MS and observed that FASN inhibition by IPI-9119 leads to a reduction in phosphatidylglycerol levels **(Figure 18B)**, an alteration that can lead to mitochondria dysfunction, as this phospholipid is a precursor in the synthesis of cardiolipin.

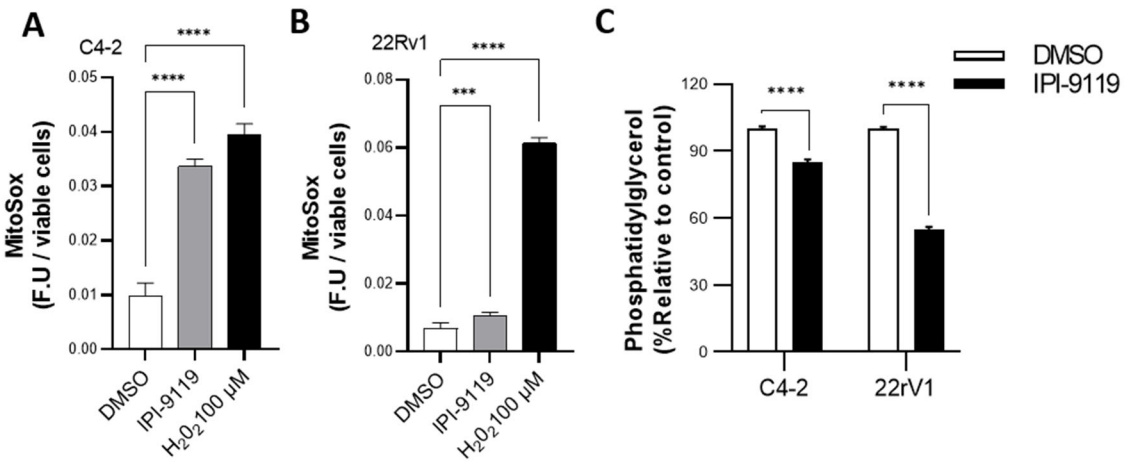

Figure 18. Superoxide levels and phospholipid modulation induced by IPI-9199 treatment in CRPC cells
A,B) Mitochondrial superoxide levels assessed by MitoSox oxidation in C4-2 or 22Rv1 cells with negative control (DMSO), IPI-9119 or positive control (hydrogen peroxide). Results expressed as relative fluorescence (510/580 nm) normalized to viable cells. Mean values ± SD, one-way ANOVA, ****p<0.0001, *** p<0.001. **C)** Total combined sum compositions of phosphatidylglycerol species. Results expressed as percentage relative to control (DMSO). Mean values ± SEM, multiple unpaired t-test with Welch correction, ****p<0.0001.

Site of performance: Weill Cornell Medical College
WCM site team: Massimo Loda (PI), Caroline F. Ribeiro (Research associate).

13. FASN inhibition alters tumor growth in LuCap 35 human PDX models.

We observed that inhibition of FASN can sensitize cells to Enzalutamide (**Figure 8**), as well as CRPC human organoids (**Figure 11**), potentiating the anti-androgen therapy. Next, we decided to evaluate the effect of this combinatorial treatment in the growth of Patient-Derived Xenograft (PDX) models. LuCap 35 castrate resistant human PDX tumors were implanted subcutaneously into SCID mice that had been previously castrated. When tumors regrew to 50-100mm^3 treatment began with vehicle, Enzalutamide at 20 mg/kg, the murine FASN inhibitor TVB-3664 (*Sagimet*) at 10mg/kg, or its combination. In total, 12 animals were included in each group. Regrowth after initial castration took 6-8 months. There was significant suppression of tumor growth in the Enzalutamide combined with TVB-3664 group compared to singe agent and vehicle groups. After 5 weeks treatment vehicle control 307 mm^3 +/- 73.6 std vs treatment 124 mm^3 +/- 8.3 std. p < 0.0005 (**Figure 19**). Tumors have been collected and will be sent for lipid metabolomic analysis as well as histology.

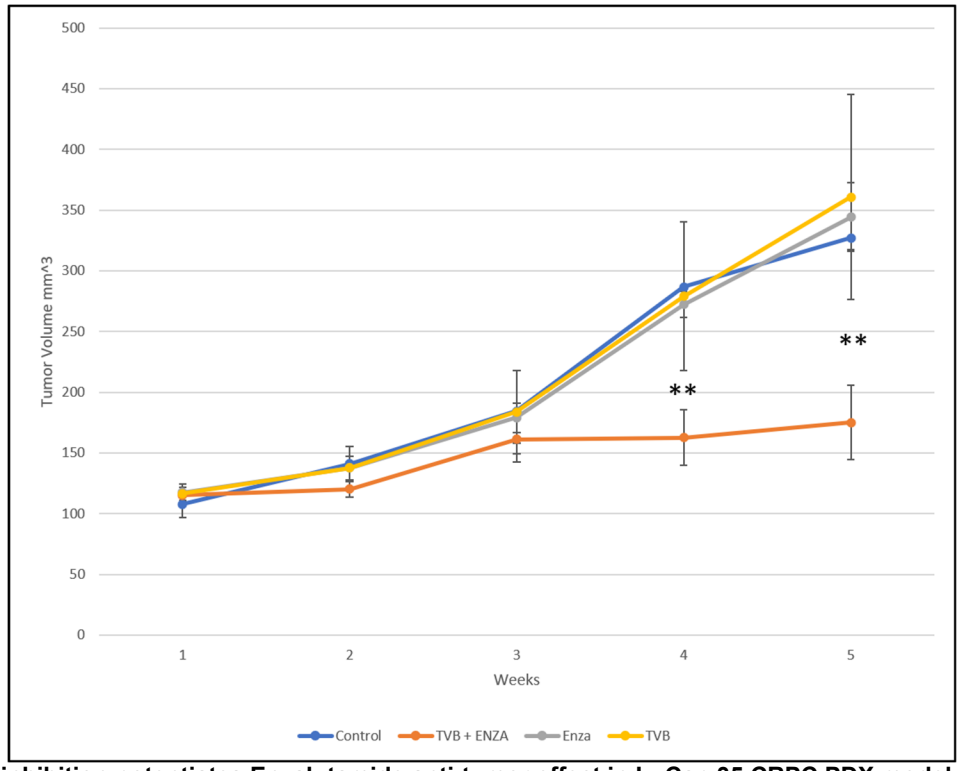

Figure 19. FASN inhibition potentiates Enzalutamide anti-tumor effect in LuCap 35 CRPC PDX model
Average tumor volume of LuCap 35 PDX during 5-week treatment with TVB-3664 and Enzalutamide (n=12). Results are expressed as n-fold the mean initial volume (equal to 1) ± SEM. (**p= 0.0016, end of treatment, Mann-Whitney non-parametric test).

Performance Site: University of Washington SLU
Team: Stephen Plymate, Takuma Uo, Kathryn Epilepsia

References:

1. de Bono JS, Logothetis CJ, Molina A, Fizazi K, North S, Chu L, Chi KN, Jones RJ, Goodman OB, Jr., Saad F, Staffurth JN, Mainwaring P, Harland S, Flaig TW, Hutson TE, Cheng T, Patterson H, Hainsworth JD, Ryan CJ, Sternberg CN, Ellard SL, Flechon A, Saleh M, Scholz M, Efstathiou E, Zivi A, Bianchini D, Loriot Y, Chieffo N, Kheoh T, Haqq CM, Scher HI, Investigators C-A-. Abiraterone and increased survival in metastatic prostate cancer. N Engl J Med. 2011;364(21):1995-2005. doi: 10.1056/NEJMoa1014618. PubMed PMID: 21612468; PMCID: PMC3471149.
2. Scher HI, Fizazi K, Saad F, Taplin ME, Sternberg CN, Miller K, de Wit R, Mulders P, Chi KN, Shore ND, Armstrong AJ, Flaig TW, Flechon A, Mainwaring P, Fleming M, Hainsworth JD, Hirmand M, Selby B, Seely L, de Bono JS, Investigators A. Increased survival with enzalutamide in prostate cancer after chemotherapy. N Engl J Med. 2012;367(13):1187-97. doi: 10.1056/NEJMoa1207506. PubMed PMID: 22894553.
3. Beer TM AA, Rathkopf DE, Loriot Y, Sternberg CN, Higano CS, Iversen P, Bhattacharya S, Carles J, Chowdhury S, Davis ID, de Bono JS, Evans CP, Fizazi K, Joshua AM, Kim CS, Kimura G, Mainwaring P, Mansbach H, Miller K, Noonberg SB, Perabo F, Phung D, Saad F, Scher HI, Taplin ME, Venner PM, Tombal B; PREVAIL Investigators. Enzalutamide in metastatic prostate cancer before chemotherapy. N Engl J Med. 2014:424-33. Epub 2014 June 1. doi: 10.1056/NEJMoa1405095; PMCID: PMC4418931.
4. Paller CJ, Antonarakis ES. Management of biochemically recurrent prostate cancer after local therapy: evolving standards of care and new directions. Clin Adv Hematol Oncol. 2013;11(1):14-23. Epub 2013/02/19. PubMed PMID: 23416859; PMCID: PMC3624708.
5. Ryan CJ, Tindall DJ. Androgen receptor rediscovered: the new biology and targeting the androgen receptor therapeutically. J Clin Oncol. 2011;29(27):3651-8. Epub 2011/08/22. doi: 10.1200/JCO.2011.35.2005. PubMed PMID: 21859989.

6. Dehm SM SL, Heemers HV, Vessella RL, Tindall DJ. Splicing of a novel androgen receptor exon generates a constitutively active androgen receptor that mediates prostate cancer therapy resistance. Cancer Res. 2008;68(13):5469-77. doi: 10.1158/0008-5472.CAN-08-0594; PMCID: PMC2663383.
7. Li Y, Chan SC, Brand LJ, Hwang TH, Silverstein KA, Dehm SM. Androgen receptor splice variants mediate enzalutamide resistance in castration-resistant prostate cancer cell lines. Cancer Res. 2013;73(2):483-9. Epub 2012/11/01. doi: 10.1158/0008-5472.CAN-12-3630. PubMed PMID: 23117885; PMCID: PMC3549016.
8. Kohli M, Ho Y, Hillman DW, Van Etten JL, Henzler C, Yang R, Sperger JM, Li Y, Tseng E, Hon T, Clark T, Tan W, Carlson RE, Wang L, Sicotte H, Thai H, Jimenez R, Huang H, Vedell PT, Eckloff BW, Quevedo JF, Pitot HC, Costello BA, Jen J, Wieben ED, Silverstein KAT, Lang JM, Wang L, Dehm SM. Androgen Receptor Variant AR-V9 Is Coexpressed with AR-V7 in Prostate Cancer Metastases and Predicts Abiraterone Resistance. Clin Cancer Res. 2017;23(16):4704-15. Epub 2017/05/06. doi: 10.1158/1078-0432.Ccr-17-0017. PubMed PMID: 28473535; PMCID: PMC5644285.
9. Chan SC, Li Y, Dehm SM. Androgen receptor splice variants activate AR target genes and support aberrant prostate cancer cell growth independent of the canonical AR nuclear localization signal. J Biol Chem. 2012;287(23):19736-49. Epub 2012/04/26. doi: 10.1074/jbc.M112.352930. PubMed PMID: 22532567.
10. Zhang X, Morrissey C, Sun S, Ketchandji M, Nelson PS, True LD, Vakar-Lopez F, Vessella RL, Plymate SR. Androgen receptor variants occur frequently in castration resistant prostate cancer metastases. PLoS One. 2011;6(11):e27970. Epub 2011/11/25. doi: 10.1371/journal.pone.0027970. PubMed PMID: 22114732; PMCID: PMC3219707.
11. Welti J, Rodrigues DN, Sharp A, Sun S, Lorente D, Riisnaes R, Figueiredo I, Zafeiriou Z, Rescigno P, de Bono JS, Plymate SR. Analytical Validation and Clinical Qualification of a New Immunohistochemical Assay for Androgen Receptor Splice Variant-7 Protein Expression in Metastatic Castration-resistant Prostate Cancer. Eur Urol. 2016;70(4):599-608. Epub 2016/04/28. doi: 10.1016/j.eururo.2016.03.049. PubMed PMID: 27117751; PMCID: PMC5015575.
12. Antonarakis ES, Lu C, Wang H, Luber B, Nakazawa M, Roeser JC, Chen Y, Mohammad TA, Chen Y, Fedor HL, Lotan TL, Zheng Q, De Marzo AM, Isaacs JT, Isaacs WB, Nadal R, Paller CJ, Denmeade SR, Carducci MA, Eisenberger MA, Luo J. AR-V7 and resistance to enzalutamide and abiraterone in prostate cancer. N Engl J Med. 2014;371(11):1028-38. Epub 2014/09/04. doi: 10.1056/NEJMoa1315815. PubMed PMID: 25184630; PMCID: PMC4201502.
13. Zadra G, Photopoulos C, Loda M. The fat side of prostate cancer. Biochim Biophys Acta. 2013;1831(10):1518-32. doi: 10.1016/j.bbalip.2013.03.010. PubMed PMID: 23562839; PMCID: PMC3766375.
14. Ettinger SL, Sobel R, Whitmore TG, Akbari M, Bradley DR, Gleave ME, Nelson CC. Dysregulation of sterol response element-binding proteins and downstream effectors in prostate cancer during progression to androgen independence. Cancer Res. 2004;64(6):2212-21. doi: 10.1158/0008-5472.can-2148-2. PubMed PMID: 15026365.
15. Rossi S, Graner E, Febbo P, Weinstein L, Bhattacharya N, Onody T, Bubley G, Balk S, Loda M. Fatty acid synthase expression defines distinct molecular signatures in prostate cancer. Mol Cancer Res. 2003;1(10):707-15. Epub 2003/08/27. PubMed PMID: 12939396.
16. Montgomery RB, Mostaghel EA, Vessella R, Hess DL, Kalhorn TF, Higano CS, True LD, Nelson PS. Maintenance of intratumoral androgens in metastatic prostate cancer: a mechanism for castration-resistant tumor growth. Cancer Res. 2008;68(11):4447-54. doi: 10.1158/0008-5472.CAN-08-0249. PubMed PMID: 18519708; PMCID: PMC2536685.
17. Little JL, Wheeler FB, Fels DR, Koumenis C, Kridel SJ. Inhibition of fatty acid synthase induces endoplasmic reticulum stress in tumor cells. Cancer Res. 2007;67(3):1262-9. Epub 2007/02/07. doi: 10.1158/0008-5472.Can-06-1794. PubMed PMID: 17283163.
18. Wu X, Dong Z, Wang CJ, Barlow LJ, Fako V, Serrano MA, Zou Y, Liu JY, Zhang JT. FASN regulates cellular response to genotoxic treatments by increasing PARP-1 expression and DNA repair activity via NF-kappaB and SP1. Proc Natl Acad Sci U S A. 2016. Epub 2016/10/30. doi: 10.1073/pnas.1609934113. PubMed PMID: 27791122; PMCID: PMC5111708.
19. Heemers HV, Verhoeven G, Swinnen JV. Androgen activation of the sterol regulatory element-binding protein pathway: Current insights. Mol Endocrinol. 2006;20(10):2265-77. Epub 2006/02/04. doi: 10.1210/me.2005-0479. PubMed PMID: 16455816.
20. Chan SC, Selth LA, Li Y, Nyquist MD, Miao L, Bradner JE, Raj GV, Tilley WD, Dehm SM. Targeting chromatin binding regulation of constitutively active AR variants to overcome prostate cancer resistance to

endocrine-based therapies. Nucleic Acids Res. 2015;43(12):5880-97. Epub 20150423. doi: 10.1093/nar/gkv262. PubMed PMID: 25908785; PMCID: PMC4499120.
21. Li X, Chen YT, Hu P, Huang WC. Fatostatin displays high antitumor activity in prostate cancer by blocking SREBP-regulated metabolic pathways and androgen receptor signaling. Mol Cancer Ther. 2014;13(4):855-66. Epub 2014/02/05. doi: 10.1158/1535-7163.Mct-13-0797. PubMed PMID: 24493696; PMCID: PMC4084917.
22. Feng B, Yao PM, Li Y, Devlin CM, Zhang D, Harding HP, Sweeney M, Rong JX, Kuriakose G, Fisher EA, Marks AR, Ron D, Tabas I. The endoplasmic reticulum is the site of cholesterol-induced cytotoxicity in macrophages. Nat Cell Biol. 2003;5(9):781-92. Epub 20030810. doi: 10.1038/ncb1035. PubMed PMID: 12907943.
23. Fu S, Yang L, Li P, Hofmann O, Dicker L, Hide W, Lin X, Watkins SM, Ivanov AR, Hotamisligil GS. Aberrant lipid metabolism disrupts calcium homeostasis causing liver endoplasmic reticulum stress in obesity. Nature. 2011;473(7348):528-31. Epub 20110501. doi: 10.1038/nature09968. PubMed PMID: 21532591; PMCID: PMC3102791.
24. Volmer R, Ron D. Lipid-dependent regulation of the unfolded protein response. Curr Opin Cell Biol. 2015;33:67-73. Epub 20141225. doi: 10.1016/j.ceb.2014.12.002. PubMed PMID: 25543896; PMCID: PMC4376399.
25. Vander Griend DJ, Antony L, Dalrymple SL, Xu Y, Christensen SB, Denmeade SR, Isaacs JT. Amino acid containing thapsigargin analogues deplete androgen receptor protein via synthesis inhibition and induce the death of prostate cancer cells. Mol Cancer Ther. 2009;8(5):1340-9. Epub 2009/05/07. doi: 10.1158/1535-7163.Mct-08-1136. PubMed PMID: 19417145; PMCID: PMC3383025.
26. Pelley RP, Chinnakannu K, Murthy S, Strickland FM, Menon M, Dou QP, Barrack ER, Reddy GP. Calmodulin-androgen receptor (AR) interaction: calcium-dependent, calpain-mediated breakdown of AR in LNCaP prostate cancer cells. Cancer Res. 2006;66(24):11754-62. doi: 10.1158/0008-5472.CAN-06-2918. PubMed PMID: 17178871.
27. Kapadia B, Nanaji NM, Bhalla K, Bhandary B, Lapidus R, Beheshti A, Evens AM, Gartenhaus RB. Fatty Acid Synthase induced S6Kinase facilitates USP11-eIF4B complex formation for sustained oncogenic translation in DLBCL. Nat Commun. 2018;9(1):829. Epub 2018/02/28. doi: 10.1038/s41467-018-03028-y. PubMed PMID: 29483509; PMCID: PMC5827760.
28. Hu R, Lu C, Mostaghel EA, Yegnasubramanian S, Gurel M, Tannahill C, Edwards J, Isaacs WB, Nelson PS, Bluemn E, Plymate SR, Luo J. Distinct transcriptional programs mediated by the ligand-dependent full-length androgen receptor and its splice variants in castration-resistant prostate cancer. Cancer Res. 2012;72(14):3457-62. Epub 2012/06/20. doi: 10.1158/0008-5472.CAN-11-3892. PubMed PMID: 22710436; PMCID: PMC3415705.
29. Hornberg E, Ylitalo EB, Crnalic S, Antti H, Stattin P, Widmark A, Bergh A, Wikstrom P. Expression of androgen receptor splice variants in prostate cancer bone metastases is associated with castration-resistance and short survival. PLoS One. 2011;6(4):e19059. Epub 2011/05/10. doi: 10.1371/journal.pone.0019059. PubMed PMID: 21552559; PMCID: PMC3084247.
30. Chen Z, Wu D, Thomas-Ahner JM, Lu C, Zhao P, Zhang Q, Geraghty C, Yan PS, Hankey W, Sunkel B, Cheng X, Antonarakis ES, Wang QE, Liu Z, Huang TH, Jin VX, Clinton SK, Luo J, Huang J, Wang Q. Diverse AR-V7 cistromes in castration-resistant prostate cancer are governed by HoxB13. Proc Natl Acad Sci U S A. 2018;115(26):6810-5. doi: 10.1073/pnas.1718811115. PubMed PMID: 29844167; PMCID: PMC6042123.
31. Park JW, Park WJ, Futerman AH. Ceramide synthases as potential targets for therapeutic intervention in human diseases. Biochim Biophys Acta. 2014;1841(5):671-81. Epub 2013/09/12. doi: 10.1016/j.bbalip.2013.08.019. PubMed PMID: 24021978.
32. Zadra G, Ribeiro CF, Chetta P, Ho Y, Cacciatore S, Gao X, Syamala S, Bango C, Photopoulos C, Huang Y, Tyekucheva S, Bastos DC, Tchaicha J, Lawney B, Uo T, D'Anello L, Csibi A, Kalekar R, Larimer B, Ellis L, Butler LM, Morrissey C, McGovern K, Palombella VJ, Kutok JL, Mahmood U, Bosari S, Adams J, Peluso S, Dehm SM, Plymate SR, Loda M. Inhibition of de novo lipogenesis targets androgen receptor signaling in castration-resistant prostate cancer. Proc Natl Acad Sci U S A. 2019;116(2):631-40. Epub 2018/12/21. doi: 10.1073/pnas.1808834116. PubMed PMID: 30578319; PMCID: PMC6329966.
33. Yamashita A, Hayashi Y, Nemoto-Sasaki Y, Ito M, Oka S, Tanikawa T, Waku K, Sugiura T. Acyltransferases and transacylases that determine the fatty acid composition of glycerolipids and the metabolism of bioactive lipid mediators in mammalian cells and model organisms. Prog Lipid Res. 2014;53:18-81. Epub 2013/10/16. doi: 10.1016/j.plipres.2013.10.001. PubMed PMID: 24125941.

What opportunities for training and professional development has the project provided?
On the DFCI/WCM site, the execution of this project allowed the members Dr. Giorgia Zadra and Dr Caroline Ribeiro to establish productive collaborations with the partners co-PIs and their groups. Due to the interdisciplinary nature of the project, Dr Ribeiro gained insights into organoid generation and preclinical models of prostate cancer, she also strengthened her expertise in biochemical analyzes of cancer metabolism and established productive collaborations with other groups in Italy and Belgium. She orally presented this study at several meetings, including the Prostate Specialized Programs of Research Excellence (SPORE) Renewal Strategy Meeting at Weill Cornell.

On University of Washington, Takuma Uo, a research Assistant Professor in Dr. Plymate's lab has had the opportunity to develop ^{13}C-glucose flux techniques as well as train undergraduate students in Seahorse ECAR analyzes.

On the University of Minnesota site, this project provided postdoctoral research training to Dr. Louisa Ho. During the performance period of this project, Dr. Ho also mentored a rotation graduate student in the Dehm Lab, Jose Valentin Lopez, who recently joined the Dehm Lab for his Ph.D. thesis training.

How were the results disseminated to communities of interest?
The results obtained have been disseminated to both specialized audience as well as a more general medical public through oral and poster communication in national conferences/retreats/seminars.

4) IMPACT

- What was the impact on the development of the principal discipline of the project?
Standard of care for metastatic castration-resistant prostate cancer (mCRPC) mainly relies on suppression of androgen receptor (AR) signaling. This approach has no lasting benefit due to the emergence of resistance mechanisms, such as ligand-independent splicing variant AR-V7. Our findings show that FASN inhibition can induce AR-V7 degradation and can potentiate AR antagonist therapy with Enzalutamide, an important therapeutic implication, especially in the CRPC setting. We also demonstrated that combining IPI-9119 with Olaparib increased therapeutic efficacy, enabling the use of PARP inhibitor therapies for prostate cancer patients that do not have BRCA1/2 mutations. Additionally, our findings have demonstrated a significant metabolic effect on FASN activity that can be inhibited by novel compounds developed at the University of Washington that specifically inhibit glycolysis in prostate cancer models. These compounds are orally bioavailable and have favorable toxicity profiles in mice. Overall, our findings could be translated to the clinic with enormous benefit on the quality of life of patients with advanced prostate cancer.

- What was the impact on other disciplines?
We have identified a mutual link between lipid metabolism and nuclear hormones, that may affect other receptors, including glucocorticoids or estrogen receptors, extending the clinical translatability to other disease types such as breast cancer. Furthermore, we have an ongoing successful protocol for organoid generation at Weill Cornell that will be used in testing of FASN inhibitors. This system can be readily applied to different cancer types, beyond prostate. We have also identified a novel cross-talk between lipid metabolism and DNA damage response, characterized by sphingolipid upregulation.

- What was the impact on technology transfer?
University of Washington: US 2018 / 0271871 A1 BUMPED KINASE INHIBITOR COMPOSITIONS AND METHODS FOR TREATING CANCER (published 27Sep2018) Demonstrates that pyrazolo-pyrimidines, such as BKI-1553, have activity on androgen-receptor positive prostate cancer including castrate-resistant prostate cancer
Weill Cornell: Nothing to Report
University of Minnesota: Nothing to report.

-What was the impact on society beyond science and technology?
The results of our study set the stage for clinical trials using FASN inhibitors as a treatment of mCRPC driven by either AR or its ligand-independent splice variants. This therapy will result in alleviation of suffering and prolonged

survival of patients with advanced prostate cancer. Potentially, because downregulation and consequent inactivation of both ligand sensitive and independent receptors of male steroid hormones can be achieved by modulating lipogenesis, it is possible that all AR-driven resistant cancers will be efficiently treated by this novel therapeutic approach. We have recently started a Phase I trial of the combination of the FASN inhibitor TVB-2640, in collaboration with *Sagimet,* with Enzalutamide to determine the RP2D for a subsequent phase II clinical trial. This study will assess pharmacokinetics (PK), pharmacodynamics (PD), safety and tolerability of TVB-2640 in combination with Enzalutamide in men with CRPC, and early sign of anti-tumor activity in this population.

5. CHANGES/PROBLEMS

- Changes in approach and reasons for change
Nothing to Report.

- Actual or anticipated problems or delays and actions or plans to resolve them.
We experienced months of delay in the execution of the research activities in all sites due to the COVID-19 pandemic in 2020, which caused suspension of laboratory work.

- Changes that had a significant impact on expenditures
Laboratory experimentation at all sites was halted and/or reduced to address the COVID-19 pandemic during 2020. This reduced expenditures on reagents and supplies for this project in YR3.

- Significant changes in use or care of human subject, vertebrate animals, biohazards, and/or selected agents
Nothing to Report

- Significant changes in use or care of human subject
Nothing to Report

- **Significant changes in use or care of vertebrate animals**
No significant changes

6. PRODUCTS

- Publications, conference papers, and presentations

Oral presentations
DFCI/WCM team
G. Zadra-Exploiting prostate cancer metabolic vulnerabilities: new therapeutic and diagnostic opportunities. Humanitas University, 2018, Milan, Italy.
G. Zadra-Targeting lipid metabolism in castration resistant prostate cancer: new therapeutic implications. Prostate Cancer Multi-Institutional Prostate Cancer Program Retreat, 2018, Fort Lauderdale, Florida.
M. Loda- Lipid metabolism in castration-resistant prostate cancer: diagnostic and therapeutic opportunities. Boston University Medical Center, 2018, Boston, MA
M. Loda- Metabolic dependencies in prostate cancer: regulation and targeting of lipogenesis. DFCI Metabolims Symposium, 2018, Boston, MA
M. Loda- Inhibition of de novo lipogenesis suppresses growth via modulation of androgen receptor signaling in CRPC. Gordon Conference, 2018.
M. Loda - Inflammation-induced suppression of cytotoxic T cell activation as a tumor promoting mechanism/ meeting, discussant. Coffey-Holden Prostate Academy Meeting, 2018, Carlsbad, CA
M. Loda - Building new bridges between basic and cancer science/symposium, chair and moderator. Pezcoller Foundation Symposium, 2018, Trento, Italy
M. Loda - Delving deeper: what we have learned from molecular characterization of prostate cancer in the TCGA Stromal signature of aggressive prostate cancer. Lipogenic prostate tumors: characterization and therapeutic

opportunities/ conference, invited Speaker. Asia Pacific Prostate Cancer Conference, 2018, Melbourne, Australia
M Loda - Panel: Hormone-Dependent Cancers-New Mechanisms and Therapeutic Targets, ENDO 2019, New Orleans, LA
M. Loda - Therapeutic Targeting of Fatty Acid Metabolism in Prostate Cancer, ENDO 2019, New Orleans, LA
M. Loda - Molecular Pathology for Cancer Researchers: Present and Future, AACR 2019 Annual Meeting, Atlanta, GA
M. Loda - Overcoming the innate resistance of cancer to therapy/ symposium; chair, moderator Pezcoller Foundation Symposium. 2019, Trento, Italy
M. Loda - PhD defense of Ali Talebi: Sustained lipogenesis as a key mediator of resistance to BRAF-targeted therapy. Thesis Committee,2019, Leuven, Belgium
M. Loda - Molecular Pathology: Past, Present and Future. NDS Research, 2019, Oxford, UK
M Loda - Role of lipids in castration-resistant prostate cancer. Invited Speaker Grand Rounds. Massachusetts General Hospital Cancer Center, Boston MA, 2020.
M Loda - Targeting of Lipid Metabolism in Prostate Cancer. Invited Speaker Grand Rounds. Mount Sinai, Dept of Urology, New York, 2020.
M Loda - Molecular Pathology for Cancer Researchers: Present and Future. AACR Annual Meeting, Atlanta, GA, 2020.
M Loda - The fat side of prostate cancer: targeting lipid metabolism. Diagnostic Pathology Course MD Anderson, Houston, TX, 2020.
C. Ribeiro - Lipid Metabolism in Prostate Cancer. Prostate Specialized Programs of Research Excellence (SPORE) Renewal Strategy Meeting at Weill Cornell. September 2020.
C. Ribeiro - FASN inhibition-induced BRCAness as a therapeutic option for castration-resistant prostate cancer (CRPC). Trainee Presentation at WCM.June, 2020.
C. Ribeiro - Inhibition of de novo lipogenesis as therapeutic option for castration-resistant prostate cancer. IFOM, Milan, Italy. July, 2019.
C. Ribeiro - Inhibition of de novo lipogenesis alters oxidative potential of prostate cancer cells. Katholieke Universiteit Leuven, Belgium. July, 2019.
M. Loda - Reprogrammed lipid metabolism in prostate cancer: therapeutic opportunities. Invited Speaker, Grand Rounds Sidney Kimmel Cancer Center at Jefferson Health. October 2020.
M. Loda - Reprogrammed lipid metabolism in prostate cancer: therapeutic opportunities. Invited Speaker Grand Rounds, Perelman School of Medicine at the University of Pennsylvania. November 2020.
M. Loda - Reprogrammed lipid metabolism in prostate cancer: therapeutic opportunities. Invited Speaker Grand Rounds, Weill Cornell. November 2020.
M Loda - Targeting lipogenesis in castration resistant prostate cancer. John Fitzpatrick Irish Genitourinary Cancer Conference. April 2021.
M. Loda - Metabolic rewiring in prostate cancer: Diagnostic and therapeutic implications. PCF Beyond Genomics WG webinar. April 2021.
S. Plymate - Prostate SPORE and PO1 presentations in Jan, March and June 2020.

Poster presentations

C.F. Ribeiro, P. Chetta, Y. Ho, S. Cacciatore, C. Photopoulos, S. Syamala, G. Xueliang, D.C. Bastos, J. Tchaicha, L. D'Anello, R., Kalekar, J. Kutok, S. Peluso, **S. Dehm, S. Plymate**, G. Zadra and **M. Loda**. Targeting androgen-receptor signaling through de novo lipogenesis inhibition in castration-resistant prostate cancer. HMS pathology retreat 2018, Boston, MA

C. F. Ribeiro, D. C. Bastos, H. Pakula, T. Ahearn, J. Nascimento, J. Clohessy, L. Mucci, S. M. Zanata, G. Zadra, **M. Loda**. Genetic and pharmacological inhibition of Fatty Acid Synthase (FASN) attenuates prostate cancer driven by Pten loss. AACR 2019 Annual Meeting, Atlanta, GA

Y. Ho, F. Vanderhoydonc, G. Zadra, C. F. Ribeiro, J. Dehairs, J. Swinnen, **M. Loda, S. Dehm**. Global changes in membrane lipid metabolism by inhibition of fatty acid synthase in prostate cancer. Abstract for 2020 Annual Conference of Society of Basic Urological Research.

Journal publications

Giorgia Zadra, Caroline F. Ribeiro, Paolo Chetta, Yeung Ho, Stefano Cacciatore, Xueliang Gao, Sudeepa Syamala, Clyde Bango, Cornelia Photopoulos, Ying Huang, Svitlana Tyekucheva, Debora C. Bastos, Jeremy Tchaicha, Brian Lawney, Takuma Uo, Laura D'Anello, Alfredo Csibi, Radha Kalekar, Benjamin Larimer, Leigh Ellis, View ORCID ProfileLisa M. Butler, Colm Morrissey, Karen McGovern, Vito J. Palombella, Jeffery L. Kutok, Umar Mahmood, Silvano Bosari, Julian Adams, Stephane Peluso, **Scott M. Dehm, Stephen R. Plymate, Massimo Loda**. Inhibition of de novo lipogenesis targets androgen receptor signaling in castration-resistant prostate cancer. PNAS, 2019 Jan 8;116(2):631-640

Harri M Itkonen, Ninu Poulose, Rebecca E Steele, Sara E S Martin, Zebulon G Levine, Damien Y Duveau, Ryan Carelli, Reema Singh, Alfonso Urbanucci, **Massimo Loda**, Craig J Thomas, Ian G Mills, Suzanne Walker. Inhibition of O-GlcNAc Transferase Renders Prostate Cancer Cells Dependent on CDK9. Mol Cancer Res, 2020 Oct;18(10):1512-1521. doi: 10.1158/1541-7786. PMID: 32611550

Syed Haider, Svitlana Tyekucheva, Davide Prandi, Natalie S. Fox, Jaeil Ahn, Andrew Wei Xu, Angeliki Pantazi, Peter J. Park, Peter W. Laird, Chris Sander, Wenyi Wang, Francesca Demichelis, **Massimo Loda**, Paul C. Boutros, and The Cancer Genome Atlas Research Network. Systematic Assessment of Tumor Purity and Its Clinical Implications. JCO Precis Oncol, 2020 Sep 4. doi: 10.1200/PO.20.00016. PMID: 33015524

Konrad H Stopsack, Ying Huang , Svitlana Tyekucheva, Travis A Gerke, Clyde Bango, Habiba Elfandy, Michaela Bowden, Kathryn L Penney, Thomas M Roberts, Giovanni Parmigiani, Philip W Kantoff, Lorelei A Mucci, **Massimo Loda**. Multiplex Immunofluorescence in Formalin-Fixed Paraffin-Embedded Tumor Tissue to Identify Single-Cell-Level PI3K Pathway Activation. Clin Cancer Res, 2020 Sep 10. doi: 10.1158/1078-0432. PMID: 32913135

Lisa M Butler, Ylenia Perone, Jonas Dehairs, Leslie E Lupien, Vincent de Laat, Ali Talebi**, Massimo Loda**, William B Kinlaw, Johannes V Swinnen. Lipids and cancer: Emerging roles in pathogenesis, diagnosis and therapeutic intervention. Adv Drug Deliv Rev, 2020 Jul 23. doi: 10.1016/j.addr.2020.07.013. PMID: 32711004

Takuma Uo, Cynthia C Sprenger, **Stephen R Plymate.** Androgen Receptor Signaling and Metabolic and Cellular Plasticity during Progression to Castration Resistant Prostate Cancer. Frontiers in Oncology 2020 Oct 9;10:580617. doi: 10.3389/fonc.2020.580617. eCollection 2020. PMID: 33163409

Débora C. Bastos, Caroline F. Ribeiro, Thomas Ahearn, Jéssica Nascimento, Hubert Pakula, John Clohessy, Lorelei Mucci, Thomas Roberts, Silvio M. Zanata, Giorgia Zadra, **Massimo Loda.** Genetic ablation of FASN attenuates the invasive potential of prostate cancer driven by Pten loss. The Journal of Pathology 2021 Mar;253(3):292-303. doi: 10.1002/path.5587. PMID: 33166087

- Website(s) or other Internet site (s)

Nothing to Report

- Technologies or techniques

Nothing to Report

- Inventions, patent applications, and/or licenses

Nothing to Report

- Other Products

Nothing to Report so far

7. PARTICIPANTS & OTHER COLLABORATING ORGANIZATIONS

a. What individuals have worked on the project?

This information is related only to Dana-Farber Cancer Institute/ Weill Cornell Medicine Performance site

Name	Massimo Loda
Project Role	PI
Research identifier	NA
Nearest person month	1 calendar (effort for last period)
Contribution to Project	Supervision of the entire project

Name	Giorgia Zadra
Project Role	Co-investigator/Instructor
Research identifier	NA
Nearest person month	3.6
Contribution to Project	Performed metabolomics/RNAseq experiments

Name	Caroline F. Ribeiro
Project Role	Research Associate
Research identifier	NA
Nearest person month	7 calendar (effort for last period)
Contribution to Project	Performed *in vitro* and *in vivo* experiments, analysis of RNAseq, metabolomics and lipidomics data

Name	Hubert Pakula
Project Role	Research Associate
Research identifier	NA
Nearest person month	2 calendar (effort for last period)
Contribution to Project	Performed *in vitro* and *in vivo* experiments, analysis of RNAseq, metabolomics and lipidomics data

Name	Madhavi Jere
Project Role	Technician
Research identifier	NA
Nearest person month	7 calendar (effort for last period)
Contribution to Project	Supported *in vitro* and *in vivo* experiments

Name	Leigh Ellis
Project Role	Co-investigator/Assistant Professor
Research identifier	NA
Nearest person month	2.4 calendar
Contribution to Project	Supervision of organoid model generation

This information is related only to the University of Washington site

Name	Stephen Plymate
Project Role	Professor
Research identifier	NA
Nearest person month	1.2
Contribution to Project	In vivo evaluation and PDX models

Name	Takuma Uo
Project Role	Assistant Professor
Research identifier	NA
Nearest person month	1.2
Contribution to Project	Supervision of organoid models, SGI data

This information is related only to the University of Minnesota site

Name	Scott Dehm
Project Role	PI
Research identifier	NA
Nearest person month	1.2
Contribution to Project	Supervision of project at University of Minnesota; coordination and communication with co-PIs Loda and Plymate

Name	Yingming Li
Project Role	Research Associate
Research identifier	NA
Nearest person month	1.2
Contribution to Project	Project assistance to Louisa Ho, laboratory management and reagent ordering, maintenance of prostate cancer models.

Name	Yeung Louisa Ho
Project Role	Postdoctoral Associate
Research identifier	NA
Nearest person month	4.8
Contribution to Project	Lipidomic profiling, investigation of mechanisms underlying IPI-9119 mediated inhibition of AR and AR-V7.